LETTERS

Edited by ***Jennifer Sills***

Retraction

SCIENCE HAS RECEIVED the results of the University of California, Riverside Committee on Privilege and Tenure's investigation of the papers published in *Science* by Professor Frank Sauer and colleagues, "TAF1 activates transcription by phosphorylation of serine 33 in histone H2B" (*1*) and "Noncoding RNAs of trithorax response elements recruit *Drosophila* Ash1 to Ultrabithorax" (*2*).

For the 2004 Report (*1*), the Committee's findings can be summarized as follows: Lanes 3 and 4 in Fig. 1B were replicated from a figure in another paper (*3*). There was manipulation of gel images that constituted data falsification and fabrication in Fig. 2C; Fig. 3, B and C; Fig. 4, B and D; and panel A in fig. S5C. For the 2006 Research Article (*2*), the Committee's findings can be summarized as follows: In Fig 6C, there was replication of the same image in two panels that constitutes data falsification. There was manipulation of gel images that constituted data falsification and fabrication in Fig. 4D; Fig. 6, A and B; and fig. S5A.

The Committee concluded that the image manipulations described above constituted a significant departure from the accepted practices of Dr. Sauer's research community. Therefore, the data, results, and conclusions in the papers are clearly not reliable. *Science* is hereby retracting the papers, at the request of University of California, Riverside and Dr. Sauer. The Committee determined that Dr. Sauer was the sole individual responsible for producing the figures.

Marcia McNutt
Editor-in-Chief

REFERENCES

1. T. Maile *et al.*, *Science* **304**, 1010 (2004).
2. T. Sanchez-Elsner *et al.*, *Science* **311**, 1118 (2006).
3. C. Beisel *et al.*, *Nature* **419**, 857 (2002).

CKDu in Sri Lanka

CHRONIC KIDNEY DISEASE of unknown cause (CKDu), seen in Central America ("Mesoamerica's mystery killer," J. Cohen, News Focus, 11 April, p. 143), has also been prevalent in Sri Lanka since the 1990s. As in Central America, those affected are predominantly male rice farmers toiling under dry, dehydrating conditions.

A recent cross-sectional study concluded that the likely culprit is chronic exposure to low levels of Cd and As through the food chain and to pesticides, along with other predisposing factors (e.g., selenium deficiency) (*1*). An unequivocal cause-and-effect explanation has remained elusive and, as in the Americas, many contributing factors have been studied, including heavy metals, pesticides, hard water, cyanotoxins, and water fluoride content (*2*, *3*).

CKDu is a recent phenomenon, whereas rice farming has taken place since ancient times in these regions without apparent health concerns. Recent changes include climate, food habits, and social lifestyle. Perhaps we should discard the conventional search for mechanistic explanations and instead take a holistic approach focusing on the environmental changes and social lifestyle of the affected communities.

M. C. M. Iqbal* *and* ***C. B. Dissanayake***

Institute of Fundamental Studies, Hantana Road, Kandy, Sri Lanka.
*Corresponding author. E-mail: mcmif2003@yahoo.com

REFERENCES

1. N. Jayatilake *et al.*, *BMC Nephrol.* **14**, 180 (2013).
2. R. Chandrajith *et al.*, *Environ. Geochem. Health* **33**, 267 (2011).
3. C. B. Dissanayake, *Geol. Soc. London Spec. Pub.* **113**, 131 (1996).

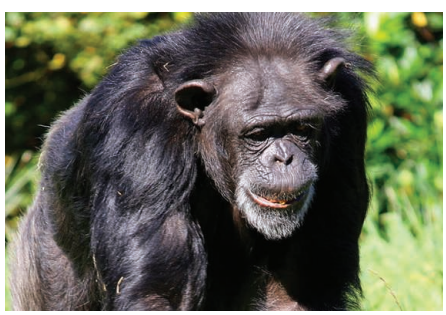

Perceived threat. Fear complicates conservation.

PHOTO: BARDROCK/WIKIMEDIA COMMONS

Fear beyond predators

IN THEIR PERSPECTIVE, "Tolerance for predatory wildlife" (2 May, p. 476), A. Treves and J. Bruskotter argue that when examining reasons for intolerance of and intention to kill predators, social factors (such as peer group norms and government-sanctioned predator killings) are more important than conventionally held views (such as measured or perceived threats to livelihoods). The authors use case studies on jaguars, wolves, lions, and bears to convincingly support their argument.

With increased anthropogenic disturbance, species not traditionally viewed as predatory may respond increasingly aggressively toward people. Although attacks are rare, concerns about sharing landscapes with great apes may be motivated more by fear of physical aggression than other more common causes of provocation such as threats to livelihoods (i.e., crop damage). As with carnivores, tolerance by local people toward these large-bodied mammals is affected by deep-rooted social beliefs that can influence outcomes, including retaliatory killings.

People's tolerance of wildlife can change quickly in response to shifting economic, demographic, and political conditions. To understand the potential for sustainable human-wildlife coexistence, human social change must be considered alongside changing wildlife behavior in response to human activities and across contexts (such as crop feeding, livestock depredation, and attacks on people) and species. To disentangle such complexities, conservation science must encourage collaborations between social and biological scientists.

Kimberley J. Hockings,[1,2]*
Matthew R. McLennan,[1] Catherine Hill[1]

[1]Social Sciences, Oxford Brookes University, Oxford, OX3 0BP, UK. [2]Centre for Research in Anthropology (CRIA), Lisbon, 1069-061, Portugal.
*Corresponding author.
E-mail: khockings@brookes.ac.uk

TECHNICAL COMMENT ABSTRACTS

Comment on "High-resolution global maps of 21st-century forest cover change"

Robert Tropek, Ondřej Sedláček, Jan Beck, Petr Keil, Zuzana Musilová, Irena Šímová, David Storch

Hansen *et al.* (Reports, 15 November 2013, p. 850) published a high-resolution global forest map with detailed information on local forest loss and gain. We show that their product does not distinguish tropical forests from plantations and even herbaceous crops, which leads to a substantial underestimate of forest loss and compromises its value for local policy decisions.

Full text at http://dx.doi.org/10.1126/science.1248753

Response to Comment on "High-resolution global maps of 21st-century forest cover change"

M. Hansen, P. Potapov, B. Margono, S. Stehman, S. Turubanova, A. Tyukavina

Tropek *et al.* critique the Hansen *et al.* global forest loss paper in terms of its utility and accuracy. Both criticisms suffer from a miscomprehension of the definition of forest employed as well as the requirements of product validation. Utility of the product is enhanced through its integration with forest type, carbon stock, protected area status, and other ancillary data.

Full text at http://dx.doi.org/10.1126/science.1248817

For northern blotting, 7 μg of RNA prepared by a standard method was loaded in each lane. Hybridizations were performed under high stringency conditions, and exposure times varied between overnight and 3 d at −80 °C with intensifying screens.

Received 24 June; accepted 12 September 2002; doi:10.1038/nature01120.
Published online 2 October 2002.

1. Sionov, R. & Haupt, Y. The cellular response to p53: the decision between life and death. *Oncogene* **18,** 6145–6157 (1999).
2. Vousden, K. H. p53: death star. *Cell* **103,** 691–694 (2000).
3. Lu, K. P., Hanes, S. D. & Hunter, T. A human peptidyl-prolyl isomerase essential for regulation of mitosis. *Nature* **380,** 544–547 (1996).
4. Sudol, M. & Hunter, T. NeW Wrinkles for an old domain. *Cell* **103,** 1001–1004 (2000).
5. Pathan, N., Aime-Sempe, C., Kitada, S., Haldar, S. & Reed, J. C. Microtubule targeting drugs induce Bcl-2 phosphorylation and association with Pin1. *Neoplasia* **3,** 70–79 (2001).
6. Shen, M., Stukenberg, P. T., Kirschner, M. W. & Lu, K. P. The essential mitotic peptidyl-prolyl isomerase Pin1 binds and regulates mitosis-specific phosphoproteins. *Genes Dev.* **12,** 706–720 (1998).
7. Winkler, K. E., Swenson, K. I., Kornbluth, S. & Means, A. R. Requirement of the prolyl isomerase Pin1 for the replication checkpoint. *Science* **287,** 1644–1647 (2000).
8. Lu, P. J., Zhou, X. Z., Shen, M. & Lu, K. P. Function of WW domains as phosphoserine- or phosphothreonine-binding modules. *Science* **283,** 1325–1328 (1999).
9. Verdecia, M. A., Bowman, M. E., Lu, K. P., Hunter, T. & Noel, J. P. Structural basis for phosphoserine-proline recognition by group IV WW domains. *Nature Struct. Biol.* **7,** 639–643 (2000).
10. Bulavin, D. V. *et al.* Phosphorylation of human p53 by p38 kinase coordinates N-terminal phosphorylation and apoptosis in response to UV radiation. *EMBO J.* **18,** 6845–6854 (1999).
11. Wang, Y. & Prives, C. Increased and altered DNA binding of human p53 by S and G2/M but not G1 cyclin-dependent kinases. *Nature* **376,** 88–91 (1995).
12. Serrano, M., Lin, A. W., McCurrach, M. E., Beach, D. & Lowe, S. W. Oncogenic ras provokes premature cell senescence associated with accumulation of p53 and p16INK4a. *Cell* **88,** 593–602 (1997).
13. de Stanchina, E. *et al.* E1A signaling to p53 involves the p19(ARF) tumour suppressor. *Genes Dev.* **12,** 2434–2442 (1998).
14. Stukenberg, P. T. & Kirschner, M. W. Pin1 acts catalytically to promote a conformational change in Cdc25. *Mol. Cell* **7,** 1071–1083 (2001).
15. Fujimori, F., Takahashi, K., Uchida, C. & Uchida, T. Mice lacking Pin1 develop normally, but are defective in entering cell cycle from G(0) arrest. *Biochem. Biophys. Res. Commun.* **265,** 658–663 (1999).
16. Lowe, S. W., Ruley, H. E., Jacks, T. & Housman, D. E. p53-dependent apoptosis modulates the cytotoxicity of anticancer agents. *Cell* **74,** 957–967 (1993).
17. Vogelstein, B., Lane, D. & Levine, A. J. Surfing the p53 network. *Nature* **408,** 307–310 (2000).
18. Bates, S. & Vousden, K. Mechanisms of p53-mediated apoptosis. *Cell Mol. Life Sci.* **55,** 28–37 (1999).
19. Wulf, G. M. *et al.* Pin1 is overexpressed in breast cancer and cooperates with Ras signalling in increasing the transcriptional activity of c-jun towards cyclin D1. *EMBO J.* **20,** 3459–3472 (2001).
20. Ryo, A., Nakamura, M., Wulf, G., Liu, Y.-C. & Lu, K. P. Pin1 regulates turnover and subcellular localization of β-catenin by inhibiting its interaction with APC. *Nature Cell Biol.* **3,** 793–801 (2001).
21. Tetsu, O. & McCormick, F. β-catenin regulates expression of cyclin D1 in colon carcinoma cells. *Nature* **398,** 422–426 (1999).
22. Damalas, A. *et al.* Excess β-catenin promotes accumulation of transcriptionally active p53. *EMBO J.* **18,** 3054–3063 (1999).
23. Kwonseop, K., Pang, K. M., Evans, M. & Hay, E. D. Overexpression of β-catenin induces apoptosis independent of its transactivation function with LEF-1 or the involvement of major G1 cell cycle regulators. *Mol. Biol. Cell* **11,** 3509–3523 (2000).
24. Park, D. S. *et al.* Cyclin-dependent kinases participate in death of neurons evoked by DNA-damaging agents. *J. Cell Biol.* **143,** 457–467 (1998).
25. Buschmann, T. *et al.* Jun NH2-terminal Kinase phosphorylation of p53 on Thr-81 is important for p53 stabilization and transcriptional activities in response to stress. *Mol. Cell. Biol.* **21,** 2743–2754 (2001).
26. Gostissa, M. *et al.* Activation of p53 by conjugation to the ubiquitin-like protein SUMO-1. *EMBO J.* **18,** 6462–6471 (1999).
27. Wu, Z. *et al.* Mutation of mouse p53 Ser23 and the response to DNA damage. *Mol. Cell. Biol.* **22,** 2441–2449 (2002).
28. Maestro, R. *et al.* Twist is a potential oncogene that inhibits apoptosis. *Genes Dev.* **13,** 2207–2217 (1999).

Supplementary Information accompanies the paper on *Nature*'s website (http://www.nature.com/nature).

Acknowledgements We thank our colleagues at the LNCIB for advice, discussions and critical reading of the manuscript; S. Piazza, F. Agostini and E. Guida for experimental support; M. Oren for suggestions and for providing the luciferase constructs; M. Serrano, B. Amati, R. Maestro, X. Lu, T. Crook and S. Soddu for supplying other reagents; G. Zambetti for advice about the preparation of mouse thymocytes; R. Vidimari and A. Beorchia for helping in γ-irradiation experiments; M. Stebel for production of MEFs and technical assistance; and J. Xiao for discussions and for sharing unpublished data. This work was supported by the Associazione Italiana per la Ricerca sul Cancro (AIRC) and MURST (PRIN Cofin 2000) (G.D.S.). M.G. is an FIRC (Fondazione Italiana per la Ricerca sul Cancro) Fellow.

Competing interests statement The authors declare that they have no competing financial interests.

Correspondence and requests for materials should be addressed to G.D.S. (e-mail: delsal@sci.area.trieste.it).

Histone methylation by the *Drosophila* epigenetic transcriptional regulator Ash1

Christian Beisel*, Axel Imhof†, Jaime Greene*‡, Elisabeth Kremmer§ & Frank Sauer*‡

** Zentrum für Molekulare Biologie der Universität Heidelberg (ZMBH), Im Neuenheimer Feld 282, 69120 Heidelberg, Germany*
† Adolf-Butenandt Institut, Universität München, Schillerstrasse 44, 80336 München, Germany
‡ Department of Biochemistry, 1447 Boyce Hall, University of California, Riverside, California 92521-0129, USA
§ GSF-Forschungszentrum, Institut für Molekulare Immunologie, Marchionistrasse 25, 81377 München, Germany

The establishment and maintenance of mitotic and meiotic stable (epigenetic) transcription patterns is fundamental for cell determination and function[1]. Epigenetic regulation of transcription is mediated by epigenetic activators and repressors, and may require the establishment, 'spreading' and maintenance of epigenetic signals[2]. Although these signals remain unclear, it has been proposed that chromatin structure and consequently post-translational modification of histones may have an important role in epigenetic gene expression[3,4]. Here we show that the epigenetic activator Ash1 (ref. 5) is a multi-catalytic histone methyl-transferase (HMTase) that methylates lysine residues 4 and 9 in H3 and 20 in H4. Transcriptional activation by Ash1 coincides with methylation of these three lysine residues at the promoter of Ash1 target genes. The methylation pattern placed by Ash1 may serve as a binding surface for a chromatin remodelling complex containing the epigenetic activator Brahma (Brm)[6], an ATPase, and inhibits the interaction of epigenetic repressors with chromatin. Chromatin immunoprecipitation indicates that epigenetic activation of *Ultrabithorax* transcription in *Drosophila* coincides with trivalent methylation by Ash1 and recruitment of Brm. Thus, histone methylation by Ash1 may provide a specific signal for the establishment of epigenetic, active transcription patterns.

Acetylation/de-acetylation, ubiquitination and methylation of histones (H1, H2A, H2B, H3, H4) have been correlated with the activation and silencing of transcription[7–10]. Histone methylation occurs predominantly at arginine and lysine residues in the amino-terminal tails of H3 and H4 (ref. 10). Arginine methylation mediates transcriptional activation by hormone receptors and probably other chromatin-dependent processes[11]. By contrast, methylation of K9 and K4 in H3 and K20 in H4 has been linked to transcriptionally inactive chromatin, and corresponding HMTases have been identified[10–14]. Methylation of H3 K4 has also been detected in transcription-competent chromatin[15,16], but the functional link between histone methylation and activation has not been dissected.

To identify HMTases that establish activation-specific methylation patterns, we used a biochemical screen that identified Ash1, a member of the trithorax group of epigenetic activators[1,5], as an HMTase. Ash1 contains a SET domain—the 'signature motif' of lysine-specific HMTases—flanked by cysteine-rich regions (pre-SET and post-SET domains)[5,10]. To confirm that Ash1 has HMTase activity, we tested the ability of recombinant Ash1 derivatives Ash1ΔN (deleted N terminus) and Ash1(SET) (containing the pre-SET, post-SET and SET domains only) to methylate histones (Fig. 1a). The Ash1 derivatives methylated H3 and, to a lesser extent, H4 in polynucleosomes and histone core octamers (Fig. 1a, b). By contrast 'free' H3 and H4 were methylated to a lesser extent compared with nucleosomes, even though free histones were present

at a fivefold excess over polynucleosomal histones or when supplemented with DNA (Fig. 1d). These results suggest that Ash1 methylates H3 and H4. As Ash1 used in the described HMTase assays was purified from eukaryotic cells, the HMTase activity of Ash1 could result from an associated rather than intrinsic activity. To test this, we subjected Ash1ΔN to protein transfer membrane assays that detect intrinsic enzymatic activities in proteins[8]. Ash1(SET) was separated by SDS–polyacrylamide gel electrophoresis (PAGE), transferred electrophoretically onto polyvinylidene fluoride (PVDF) membrane, and denatured/re-natured. Reconstituted Ash1(SET) methylated H3 and H4 (Fig. 1e), suggesting that Ash1 has intrinsic HMTase activity.

To identify the target amino acid residue(s) of Ash1, radiolabelled H3 was subjected to Edman-degradation. Scintillation counting of the released amino acid fractions detected radiolabelling of H3 K4 and K9 (Fig. 2a). To support this, we tested the ability of Ash1ΔN to methylate peptides consisting of amino acids 1–20 of H3 (H3(1–20)). Ash1ΔN methylated the peptides H3(1–20), H3(1–20)K4 (which contains H3 K4 but leucine residues instead of lysine residues at positions 9, 14 and 18) and H3(1–20)K9 (which contains H3 K9 but leucine residues instead of lysine residues at positions 4, 14 and 18) (Fig. 2b). By contrast, H3(1–20)L4/L9 peptides, which contain leucine residues at position 4 and 9 of H3, were not significantly methylated (Fig. 2b), indicating further that Ash1 methylates H3 K4 and K9. Owing to the weak radiolabelling, the target(s) of Ash1 in H4 could not be identified by Edman-degradation (data not shown). As H4 K20 is the only H4 residue being methylated *in vivo*, we generated a monoclonal antibody against dimethylated H4 K20 (anti-dim(H4-K20)) to investigate whether Ash1 methylates H4 K20 (refs 10, 14). H4 that was free, in histone core octamers or polynucleosomes, was methylated by Ash1 and analysed by western blot analysis. Anti-dim(H4-K20) antibody recognized Ash1-methylated H4, but not un-methylated H4, indicating that Ash1 methylates H4 K20 (Fig. 2c, d).

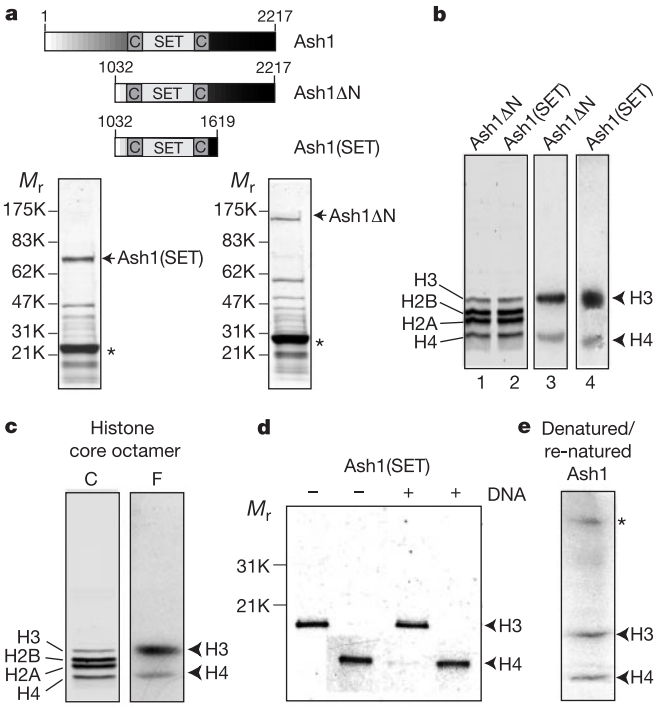

Figure 1 Ash1 methylates histone H3 and H4. **a**, Schematic representation of Ash1 derivatives (top panel). Numbers refer to amino acids in Ash1 (see GI17737643; http://www.ncbi.nlm.nih.gov). The SET domain (SET) and the cysteine-rich pre-SET and post-SET domains (C) are indicated. The bottom panel shows Coomassie-blue-stained SDS–PAGE gels of immunopurified Ash1(SET) and Ash1ΔN, whose position is indicated. The asterisk marks the position of the anti-Flag antibody light chain. **b**, Coomassie-blue-stained SDS–PAGE gel (lanes 1, 2) and fluorograms (lanes 3, 4) of HMTase assays programmed with polynucleosomes and Ash1ΔN (lanes 1, 3) or Ash1(SET) (lanes 2, 4). **c**, Coomassie-blue-stained SDS gel (C) and corresponding fluorogram (F) of an HMTase assay as in **b**, except that reactions contained histone core octamers and Ash1ΔN. **d**, Fluorogram of HMTase assays programmed with Ash1(SET) and either H3 or H4 in the absence or presence of DNA. **e**, Fluorogram of an HMTase assay programmed with polynucleosomes and protein transfer membrane-bound, denatured/re-natured Ash1(SET). An asterisk marks the position of auto-methylated Ash1(SET). The position of histones (**b**–**e**) and the position and relative molecular mass (M_r, K) of protein standards is indicated (**a**, **d**).

Single amino acid point mutations *ash1*^{10} and *ash1*^{21} abolish Ash1 activator function in *Drosophila* (ref. 5). The mutation in *ash1*^{10} (N1458I) resides within the SET domain, and in *ash1*^{21} (E1357K) in the pre-SET domain (ref. 5). To assess whether these mutations affect HMTase activity, we expressed and purified recombinant proteins containing one of these mutations (Ash1ΔN^{10}, Ash1ΔN^{21}) and a third mutant (Ash1ΔN^{1142}) whose mutation (H1459K) resides in the SET domain and abolishes HMTase activity of SUV39H1 (ref. 12). HMTase assays revealed that the mutants did not significantly methylate H3 and H4, indicating that the mutations abolish HMTase activity (Fig. 2e) and that both the pre-SET and SET domains of Ash1 contribute to HMTase activity and transcriptional activation by Ash1.

To assess whether the mutations in Ash1 specifically inactivate HMTase activity or cause a general functional inactivation, we investigated the ability of mutant Ash1ΔN to bind the known interaction partner Trx. Ash1ΔN and the three mutants interacted with Trx *in vitro* (see Supplementary Information), suggesting that the inability of mutant Ash1 proteins to methylate histones is based on a specific inactivation of HMTase activity.

To investigate the effect of *ash1*^{10} and *ash1*^{21} on transcriptional activation by Ash1 in *Drosophila*, we used transgenic flies carrying the Ash1-dependent reporter gene *N18/15*, which contains a 4-kilobase (kb) regulatory element of the *bxd* region from the Ash1 target gene *Ubx* fused to the mini-*white* gene (Fig. 2f)[17]. Ash1 supports activation of *N18/15* transcription in the *Drosophila* eye (Fig. 2f). By contrast, *N18/15* expression is significantly reduced in *ash1*^{10}/+ or *ash1*^{21}/+ heterozygous flies (Fig. 2f). As Ash1^{21} and Ash1^{10} lack HMTase activity *in vitro*, these results imply that HMTase activity contributes to transcriptional activation by Ash1 *in vivo*.

To dissect the functional relationship between transcriptional activation and histone methylation by Ash1, we reconstituted transcriptional activation by Ash1 in *Drosophila* S2 cells. To monitor transcription in chromatin, we generated S2 (BCAT5) cells that carry the stable integrated reporter gene *BCAT5*, which contains five DNA-binding sites for the yeast activator Gal4, a core promoter and the bacterial *cat* gene[18,19]. To recruit Ash1 to chromatin, Ash1 derivatives were fused to the Gal4 DNA-binding domain (amino acids 1–147) (Gal4(DBD))[20]. BCAT5 cells were transfected with plasmids expressing fusion proteins comprising Gal4(DBD) and either wild type or mutant Ash1ΔN. Gal4(DBD)–Ash1ΔN activates *BCAT5* expression 20-fold (Fig. 3a)[20], whereas HMTase-inactive Ash1ΔN derivatives did not (Fig. 3a). These results support the hypothesis that HMTase activity of Ash1 mediates activation of transcription.

To link transcriptional activation by Ash1 to histone methylation, we used crosslinked chromatin immunoprecipitation (XChIP)[21], which detects protein–DNA interactions *in vivo*. Crosslinked chromatin was isolated from BCAT5 cells expressing Gal4(DBD)–Ash1ΔN, Gal4(DBD)–Ash1ΔN^{10} or Gal4(DBD)–Ash1ΔN^{21}, and immunoprecipitated by antibodies recognizing dimethylated H3 K4, H3 K9 or H4 K20. Precipitated DNA was purified and the enhancer/promoter of target genes was detected by polymerase chain reaction (ref. 21). All three antibodies precipitated chromatin

containing the *BCAT5* enhancer/promoter from cells in which Gal4(DBD)–Ash1ΔN activates transcription (Fig. 3b). Methylation of these lysine residues was detectable 500 bp upstream of the enhancer/promoter and at the 3′-end of the *cat* gene (data not shown). In cells expressing Gal4(DBD)–Ash1ΔN[10], methylation of H3 K4 was undetectable, but weak methylation of H3 K9 and H4 K20 could be observed. This finding supports current models proposing that transcriptional repression correlates with methylation of H3 K9 and H4 K20 (refs 10–14). As, however, H3 K9 and H4 K20 methylation is enhanced at the transcriptionally active (active) reporter, transcriptional activation by Ash1 correlates with *de novo* methylation of not only H3 K4 but also H3 K9 and H4 K20.

Methylation of H3 K9 at the transcriptionally silent (silent) enhancer/promoter implied that *BCAT5* might be associated with HP1, which binds methylated H3 K9. We tested this by XChIP using anti-HP1 polyclonal antibody. The antibody precipitated the *BCAT5* enhancer/promoter from cells expressing HMTase-inactive Gal4(DBD)–Ash1ΔN[10]. By contrast, the enhancer/promoter was only weakly precipitated from cells in which Gal4(DBD)–Ash1ΔN activates reporter expression (Fig. 3b). These results suggest that HP1 binds the silent enhancer/promoter and is removed/relocated from the reporter by Ash1-mediated histone methylation.

To investigate whether Ash1 methylates histones to activate transcription of a natural target gene, we monitored methylation of *Ubx* in BCAT5 cells. *Ubx* is not expressed in S2-cells[24] but PCR with reverse transcription (RT–PCR) indicates that transiently expressed Gal4(DBD)–Ash1ΔN activates expression of this gene in BCAT5 cells (Fig. 3c). XChIP experiments indicate that H3 K4 is not methylated and that H3 K9 and H4 K20 are only weakly methylated at the silent *Ubx* promoter (Fig. 3b). By contrast, methylation of all three lysine residues is significantly enhanced when Ash1 activates *BCAT5* expression (Fig. 3b), indicating that transcriptional activation of *Ubx* by Ash1 coincides with methylation of H3 K4, K9 and H4 K20.

Genetic data indicate that Ash1 activates *Ubx* expression in imaginal discs of the third leg[25]. Therefore, to investigate histone methylation by Ash1 in the natural context of the activator, we examined the methylation pattern of *Ubx* in third leg discs by XChIP. We prepared crosslinked chromatin from third leg discs dissected from third instar larvae. Chromatin immunoprecipitations indicated methylation of H3 K4, K9 and H4 K20 at the *Ubx* promoter (Fig. 3d), suggesting that Ash1-mediated methylation of all three lysine residues coincides with epigenetic activation of *Ubx* transcription in *Drosophila*.

On the basis of the result that methylated lysine residues facilitate or inhibit the binding of proteins, we investigated whether the trivalent (H3 K4, K9 and H4 K20) methylation pattern placed by

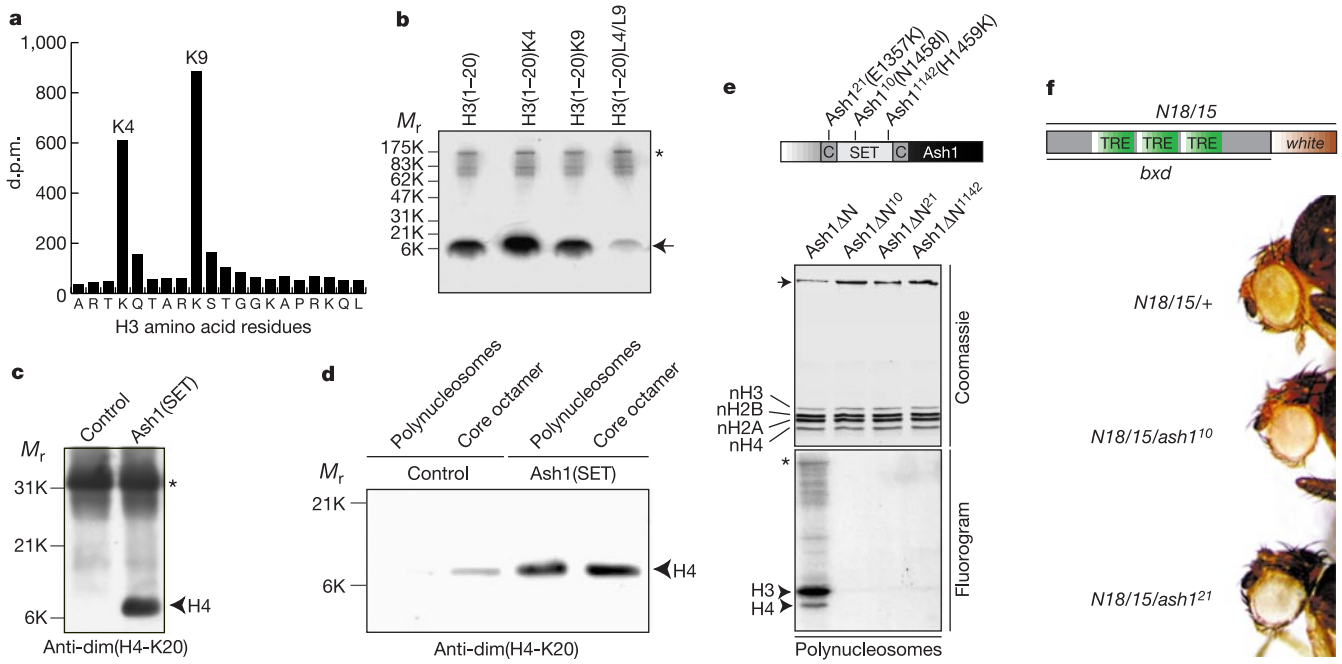

Figure 2 Ash1 methylates K4 and K9 in H3 and K20 in H4. **a**, Microsequencing of radiolabelled polynucleosomal H3. Radiolabelled H3 was subjected to Edman-degradation and the resulting amino acid fractions were analysed by scintillation counting. The *x* axis shows amino acids 1–20 of H3, the *y* axis indicates the [^{3}H]-incorporation of individual amino acids in decays per minute (d.p.m.). **b**, HMTase assays using Ash1(SET) and wild-type or mutant H3 peptides (amino acids 1–20). H3(1–20)K4, peptide containing H3 K4 only; H3(1–20)K9, peptide containing H3 K9 only; H3(1–20)L4/L9, peptide containing leucine instead of lysine at positions 4 and 9. The arrow indicates the position of radiolabelled peptide; the asterisk marks auto-methylated Ash1(SET). **c**, Western blot analyses using anti-dimethylated H4 K20 monoclonal antibody (dim(H4-K20)) of HMTase assays containing recombinant H4 and the control protein TAF$_{II}$110 or Ash1(SET). The asterisk indicates the position of anti-Flag antibody light chain. **d**, Western blot analyses as in **c**, except that reactions were programmed with polynucleosomes or histone core octamers, as indicated. The position and relative molecular mass of protein standards is indicated. Note the low basal level of H4 K20 methylation of histone core octamers. **e**, Schematic representation of mutant ASH1ΔN proteins (top). The position and the single amino acid exchange caused by the mutations are indicated. The bottom panel shows a Coomassie-blue-stained SDS gel (top) and fluorogram (bottom) of HMTase assays programmed with the indicated Ash1 derivatives and polynucleosomes. The arrow marks the position of Ash1 derivatives. The asterisk marks auto-methylated Ash1. **f**, Schematic representation of the *N18/15* reporter gene containing the 4-kb regulatory element of the *bxd* region, which contains three Trx response elements (TRE), fused to the *Drosophila* mini-*white* gene (top). The bottom panel shows photographs of eyes from *N18/15*/+ (top), *N18/15/ash1*^{10} (middle) and *N18/15/ash1*^{21} heterozygotes (bottom). Magnification, tenfold.

Ash1 attracts or repels proteins to establish epigenetic activation. The XChIP experiments in Fig. 3b, d indicate that the trivalent methylation pattern removes/relocates HP1 from chromatin. To support this finding, we investigated the interaction of HP1 with methylated H3 peptides and histone core octamers that had been methylated by Ash1 or *Drosophila* SU(VAR)3-9, which methylates H3 K9. HP1 bound H3 K9-methylated peptides and histone core octamers, as well as H3 K4/K9-methylated peptides (Fig. 4a, c). By contrast, HP1 did not bind Ash1-methylated core octamers, suggesting that the trivalent methylation pattern inhibits the interaction of HP1 with chromatin (Fig. 4b).

Protein–protein interaction assays using H3(1–20) peptides methylated at H3 K4, K9 or H3 K4 and K9 (H3 K4/K9), and *Drosophila* embryonic nuclear extract or recombinant proteins, resulted in the identification of three proteins that exhibit differential binding to methylated peptides. Two of these proteins—the epigenetic repressor Polycomb (Pc) and Caf-1 p55, a subunit of different protein complexes involved in, for example, epigenetic repression[26,27]—bind H3 K9-methylated peptides and histone core octamers, but show significantly reduced binding to H3 K4- or H3 K4/K9-methylated peptides and trivalently methylated histone core octamers (Fig. 4a, b, d–f). Furthermore, protein-binding assays indicate that Brm and Moira (Mor) interact with H3 K4/K9-methylated peptides (Fig. 4g, h). In contrast, both proteins were not recruited to peptides methylated at H3 K4 or H3 K9 (Fig. 4g, h). Brm and Mor are subunits of a SWI/SNF-like chromatin remodelling complex[1], suggesting that this complex, rather than individual proteins, is recruited to K4/K9-methylated H3. These results imply that the trivalent methylation pattern established by Ash1 facilitates or prevents the interaction of proteins with methylated H3 during epigenetic activation. To support this finding, we used XChIP to investigate the interaction of Brm and repressors with Ash1 target genes. These analyses indicate that Brm and Mor are present at the active but not at silent promoters of Ash1 target genes in cells or third leg imaginal discs (Fig. 3b, d). By contrast, the repressors were only detected at silent promoters (Fig. 3b, d). Thus, transcriptional activation by Ash1 may coincide with the recruitment of Brm and Mor and the extinction of repressor binding at the promoter of Ash1 target genes.

Collectively, our data indicate that the epigenetic activator Ash1 activates transcription by methylation of H3 K4, K9 and H4 K20 at the promoter of target genes. This suggests that epigenetic activation and silencing, which has been linked to methylated H3 K9, may correlate with different histone methylation patterns. Each of the three lysine residues targeted by Ash1 can be individually methylated by specific HMTases, resulting in transcriptional repression and probably activation (H3 K4). Combining these three modifications results in a novel biological readout: epigenetic activation. Why does the trivalent modification pattern generated by Ash1 mediate epigenetic activation? Our results indicate that each modification of the pattern fulfils a specific function. Methylation of H3 K4 prevents the interaction of repressors (Pc, p55) with Ash1 target genes. Methylation of H4 K20 in addition to H3 K4 and H3 K9 prevents the interaction of HP1 with chromatin. Inhibition of repressor binding is an important mechanism, as epigenetic activators and repressors are expressed together during *Drosophila* development. Finally, methylation of H3 K4 and H3 K9 generates an interaction surface for a chromatin-remodelling complex. Our results imply that a specific functional interplay between the epigenetic activators Ash1 and Brm mediates epigenetic activation of transcription. Ash1 initially binds target genes and generates the trivalent histone methylation pattern, which subsequently recruits a

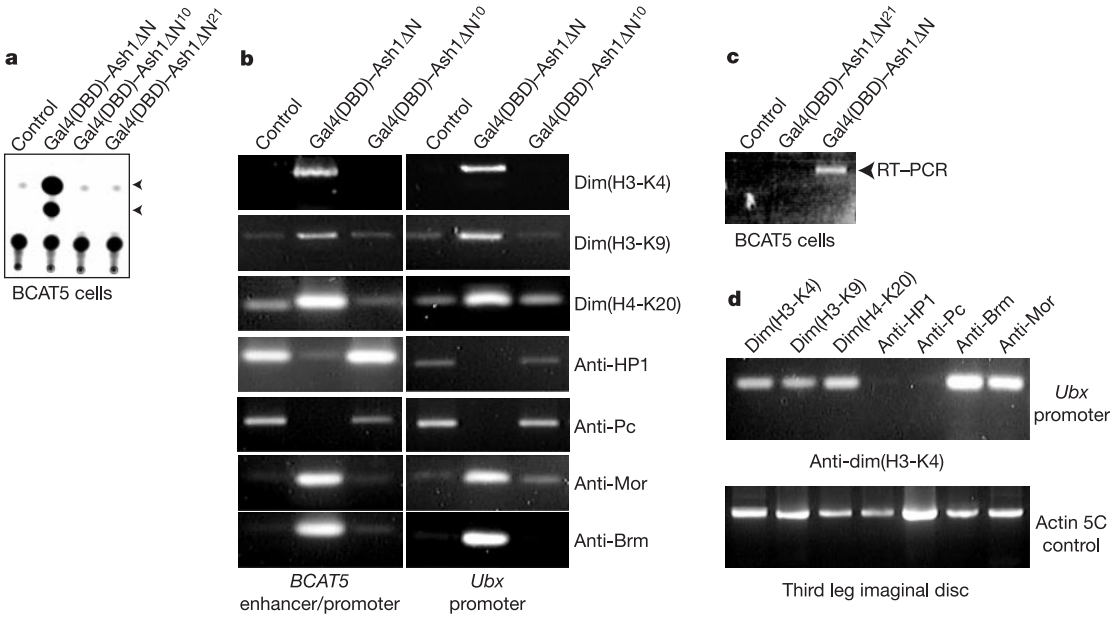

Figure 3 Methylation of K4 and K9 in H3 and K20 in H4 coincides with epigenetic activation of transcription by Ash1. **a**, Autoradiogram of CAT assays using whole-cell extract prepared from BCAT5 cells transfected with plasmids expressing the co-activator $TAF_{II}110$ (ref. 28) (control, lane 1), Gal4(DBD)–Ash1ΔN (lane 2), Gal4(DBD)–Ash1ΔN^{10} (lane 3) or Gal4(DBD)–Ash1ΔN^{21} (lane 4). The arrowheads indicate the position of acetylated [^{14}C]chloramphenicol. **b**, Photograph of ethidium-bromide-stained agarose gels containing PCR-amplified DNA obtained from XChIP experiments. *In vivo* crosslinked chromatin was isolated from BCAT5 cells that express $TAF_{II}110$ (control) or the indicated Ash1 derivatives. Crosslinked chromatin was immunoprecipitated using the indicated antibodies. PCR was used to detect a 270-bp fragment of the *BCAT5* enhancer. **c**, Ethidium-bromide-stained agarose gel of RT–PCR reactions containing PCR primers generating a 330-bp fragment of the *Ubx* coding region and DNA that was isolated from BCAT5 cells expressing $TAF_{II}110$ (control) or the indicated Ash1 derivatives. **d**, The top panel shows XChIP experiments as in **b**, but using *in vivo* crosslinked chromatin prepared from imaginal discs of the third leg of *Drosophila*. Shown is the photograph of PCR reactions detecting a *Ubx* promoter fragment in chromatin that had been immunoprecipitated using the indicated antibodies. The bottom panel is a photograph of PCR reactions that detect the presence of the actin 5C promoter in *in vivo* crosslinked chromatin using anti-dim(H3-K4) antibodies (Upstate). Precipitation of the actin 5C promoter was used to standardize PCR reactions shown in the top panel.

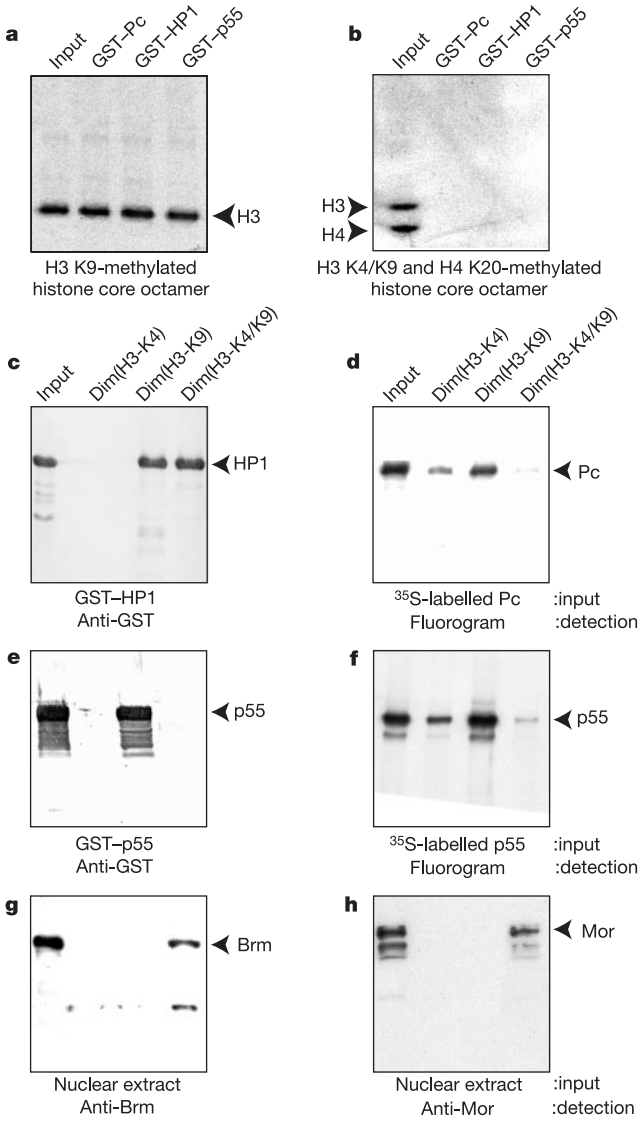

Figure 4 The trivalent methylation pattern generated by Ash1 recruits a Brm-containing chromatin remodelling factor. **a**, Fluorogram of protein–protein interaction assays containing glutathione sepharose loaded with fusion proteins consisting of GST and HP1, Pc or p55, and histone core octamers methylated at H3 K9. **b**, Same as **a**, except that histone core octamers methylated at H3 K4, H3 K9 and H4 K20 by Ash1 were used. **c**–**h**, Protein–protein interaction assays using H3 peptides (amino acids 1–20) dimethylated at H3 K4 (dim(H3-K4)), H3 K9 (dim(H3-K9)) or both (dim(H3-K4/K9)). **c**, GST–HP1; **d**, *in vitro* expressed ^{35}S-labelled Pc; **e**, GST–p55; **f**, *in vitro* expressed ^{35}S-labelled p55; **g**, **h**, *Drosophila* nuclear extract. Bound proteins were separated by SDS–PAGE and detected as indicated. Input is 10% of the input material. The position of H3 and H4 is indicated.

Brm-containing chromatin-remodelling complex. The activity of this complex may contribute to the establishment of epigenetic active chromatin structures. □

Methods

Plasmids

Expression plasmids were constructed as described in Supplementary Information. Proteins were expressed and purified as described[28].

Crosslinked chromatin immunoprecipitation

XChIP was performed essentially as described[21] with the following modifications. We used either 750 third leg imaginal discs or 4×10^7 BCAT5 cells that were transfected with plasmids expressing wild-type or mutant Gal4(DBD)–Ash1 fusion proteins. At 60 h after transfection, cells were collected and crosslinked with 1.8% formaldehyde. Crosslinked chromatin was purified as described[21]. Chromatin was immunoprecipitated using anti-dimethylated H3 K4 (dim(H3-K4)), anti-dimethylated H3 K9 (dim(H3-K9)) (both Upstate Biotechnology), and anti-dimethylated H4 K20 (dim(H4-K20)), as well as anti-HP1 anti-Pc, anti-Brm and anti-Mor antibodies. After immunoprecipitation, crosslinked chromatin was incubated with proteinase K (0.5 mg ml^{-1}) at 37 °C for 16 h. Next, crosslink was reversed by incubation of the probe at 65 °C for 6 h. DNA was purified by phenol/chloroform extraction, precipitated with ethanol, and resuspended in 100 μl TE (10 mM Tris (pH 8.0), 1 mM EDTA). For quantitative PCR we used 1/500–1/20 of the precipitated DNA. The presence of a 720-bp fragment from the constitutive active actin 5C promoter, which is methylated at H3 K4, K9 and H4 K20, was detected by PCR to normalize the precipitates obtained from XChIP (C.B. and F.S., unpublished results).

Fly strains

The following fly strains were used: *OregonR* (Bloomington stock centre), *ash1*^{10}, *ash1*^{21} (ref. 5) and *N18/15/N18/15* that contains the *N18/15* transgene (ref. 17). Flies were maintained under standard conditions. To assess the effect of *ash1*^{10} and *ash1*^{21} on the *N18/15* transgene, *N18/15/N18/15* females were crossed with w^{1118}; *ash1*^{10}/ +, w^{1118}; *ash1*^{21}/ + or w^{1118}; +/+ males and the eye colour of progenies was analysed. To exclude variations of eye colour resulting from age differences of the flies, we compared the eye colour of 3-day-old progenies expressing wild-type or mutant Ash1. Eyes are shown at a 100-fold magnification and were photographed using a standard dissection binocular.

In vitro histone methyltransferase assay

Methyltransferase assays were performed as described (ref. 16). Ash derivatives were incubated in methyltransferase buffer (25 mM Tris, pH 8.0, 100 mM NaCl, 1 mM phenylmethylsulphonyl fluoride) in the presence of 2 μCi *S*-adenosyl-L[methyl-^{3}H]-methionine (50–62 mCi mmol^{-1}) for 1 h at 30 °C. Reactions contained approximately 0.1–0.5 μg wild-type and mutant Ash1 derivatives and 1–3 μg polynucleosomal histones, 5–10 μg recombinant histones or 10 μg histone peptides.

Protein microsequencing

To determine the target amino acids of Ash1 in H3, Ash1-labelled nucleosomal H3 was subjected to microsequencing and fractions containing individual amino acid residues were analysed by scintillation counting as described[16].

In vitro protein-binding assays

Ash1 derivatives, labelled with 35S-labelled methionine, Pc and p55 were generated by *in vitro* expression[28]. Glutathione *S*-transferase (GST)–HP1, GST–p55, GST–Pc and GST–Trx(SET) were expressed and purified by affinity chromatography using glutathione-sepharose (Amersham/Pharmacia) according to the manufacturer's instructions[28]. Protein–protein interaction assays involving Trx were performed as described[17]. Binding assays involving H3 peptides were performed as described[22,23] using *in vitro* expressed proteins or fractionated embryonic *Drosophila* nuclear extract, prepared as described[28], as protein source. The identity of bound proteins was detected by western blot analyses as described[6].

Drosophila tissue culture

Drosophila S2 Schneider cells were maintained and transfected with DNA as described[20], and cells containing a stable *BCAT5* reporter gene were generated[19]. CAT assays were performed as described[20].

Preparation of polynucleosomes

Polynucleosomes were prepared from nuclei essentially as described[28] with the following modifications: after nuclease digestion, the chromatin-containing supernatant was dialysed against TE-600 (10 mM Tris, pH 8.0, 0.1 mM EDTA, 600 mM NaCl) and further purified by gel filtration using a Superdex-200 column. Polynucleosomes used in methyltransferase assays contained on average 2–20 nucleosomes.

Received 10 July; accepted 16 September 2002; doi:10.1038/nature01126.
Published online 9 October 2002.

1. Simon, J. A. & Tamkun, J. W. Programming off and on states in chromatin: mechanisms of Polycomb and trithorax group complexes. *Curr. Opin. Genet. Dev.* **12,** 210–218 (2002).
2. Urnov, F. D. & Wolffe, A. P. Above and within the genome: epigenetics past and present. *J. Mammary Gland Biol. Neoplasia* **6,** 153–167 (2001).
3. Turner, B. M. Histone acetylation and an epigenetic code. *Bioessays* **22,** 836–845 (2000).
4. Cavalli, G. & Paro, R. Epigenetic inheritance of active chromatin after removal of the main transactivator. *Science* **286,** 955–958 (1999).
5. Tripoulas, N. A., Hersperger, E., La Jeunesse, D. & Shearn, A. Molecular genetic analysis of the *Drosophila melanogaster* gene absent, small or homeotic discs1 (*ash1*). *Genetics* **137,** 1027–1038 (1994).
6. Elfring, L. K. *et al.* Genetic analysis of brahma: the *Drosophila* homolog of the yeast chromatin remodeling factor SWI2/SNF2. *Genetics* **148,** 251–265 (1998).
7. Kuo, M. H. & Allis, C. D. Roles of histone acetyltransferases and deacetylases in gene regulation. *Bioessays* **20,** 615–626 (1998).
8. Pham, A.-D. & Sauer, F. Ubiquitin-activating/conjugating activity of $TAF_{II}250$, a mediator of activation of gene expression in *Drosophila*. *Science* **289,** 2357–2360 (2000).
9. Sun, Z. W. & Allis, C. D. Ubiquitination of histone H2B regulates H3 methylation and gene silencing in yeast. *Nature* **418,** 104–108 (2002).
10. Zhang, Y. & Reinberg, D. Transcription regulation by histone methylation: interplay between different covalent modifications of the core histone tails. *Genes Dev.* **15,** 2343–2360 (2001).

11. Stallcup, M. R. Role of protein methylation in chromatin remodeling and transcriptional regulation. *Oncogene* **20,** 3014–3020 (2001).
12. Rea, S. *et al.* Regulation of chromatin structure by site-specific histone H3 methyltransferases. *Nature* **406,** 593–599 (2000).
13. Briggs, S. D. *et al.* Histone H3 lysine 4 methylation is mediated by Set1 and required for cell growth and rDNA silencing in *Saccharomyces cerevisiae*. *Genes Dev.* **15,** 3286–3295 (2001).
14. Nishioka, K. *et al.* PR-Set7 is a nucleosome-specific methyltransferase that modifies lysine 20 of histone H4 and is associated with silent chromatin. *Mol. Cell* **9,** 1201–1213 (2002).
15. Nishioka, K. *et al.* Set9, a novel histone H3 methyltrnsferase that facilitates transcription by precluding histone tail modifications required for heterochromatin formation. *Genes Dev.* **16,** 479–489 (2002).
16. Strahl, B. D., Ohba, R., Cook, R. G. & Allis, C. D. Methylation of histone H3 at lysine 4 is highly conserved and correlates with transcriptionally active nuclei in *Tetrahymena*. *Proc. Natl Acad. Sci. USA* **96,** 14967–14972 (1999).
17. Rozovskaia, T. *et al.* Trithorax and ASH1 interact directly and associate with the trithorax group-responsive *bxd* region of the Ultrabithorax promoter. *Mol. Cell. Biol.* **19,** 6441–6447 (1999).
18. Lillie, J. W. & Green, M. R. Transcription activation by the adenovirus E1a protein. *Nature* **338,** 39–44 (1989).
19. Rio, D. C. & Rubin, G. M. Transformation of cultured *Drosophila melanogaster* cells with a dominant selectable marker. *Mol. Cell. Biol.* **5,** 1833–1838 (1985).
20. Sauer, F. & Jäckle, H. Dimerization and the control of transcription by Krüppel. *Nature* **364,** 454–457 (1993).
21. Kuo, M. H. & Allis, C. D. *In vivo* cross-linking and immunoprecipitation for studying dynamic Protein:DNA associations in a chromatin environment. *Methods* **19,** 425–433 (1999).
22. Bannister, A. J. *et al.* Selective recognition of methylated lysine 9 on histone H3 by the HP1 chromo domain. *Nature* **410,** 120–124 (2001).
23. Lachner, M., O'Carroll, D., Rea, S., Mechtler, K. & Jenuwein, T. Methylation of histone H3 lysine 9 creates a binding site for HP1 proteins. *Nature* **410,** 116–120 (2001).
24. Orlando, V. & Paro, R. Mapping Polycomb-repressed domains in the *bithorax complex* using *in vivo* formaldehyde cross-linked chromatin. *Cell* **75,** 1187–1198 (1993).
25. LaJeunesse, D. & Shearn, A. Trans-regulation of thoracic homeotic selector genes of the Antennapedia and bithorax complexes by the trithorax group genes: absent, small, and homeotic discs 1 and 2. *Mech. Dev.* **53,** 123–139 (1995).
26. Paro, R. & Hogness, D. S. The Polycomb protein shares a homologous domain with a heterochromatin-associated protein of *Drosophila*. *Proc. Natl Acad. Sci. USA* **88,** 263–267 (1991).
27. Ridgway, P. & Almouzni, G. CAF-1 and the inheritance of chromatin states: at the crossroads of DNA replication and repair. *J. Cell Sci.* **113,** 2647–2658 (2000).
28. Sauer, F., Hansen, S. K. & Tjian, R. DNA template and activator-coactivator requirements for transcriptional synergism by *Drosophila* Bicoid. *Science* **270,** 1825–1828 (1995).

Supplementary Information accompanies the paper on *Nature*'s website (**http//www.nature.com/nature**).

Acknowledgements We thank M. Meisterernst for anti-dimethylated H4-K20 antibody; A. Shearn and A. Mazo for fly strains; R. Deuring and J. Tamkun for anti-Brm antibody; S. Schönfelder and R. Paro for Trx cDNA; J. Tyler for p55 cDNA; and various members of the laboratory for critical reading of the manuscript. We are grateful to J. Rami for editorial help and Y. Cully for photowork. This work was supported by a Graduiertenkolleg 484 fellowship (Deutshe Forschungsgemeinschaft) (C.B.) and a Tranregio/Sonderforschungsbereich grant (F.S.).

Competing interests statement The authors declare that they have no competing financial interests.

Correspondence and requests for materials should be addressed to F.S. (e-mail: f.sauer@mail.zmbh.uni-heidelberg.de).

erratum

Self-organization of supramolecular helical dendrimers into complex electronic materials

V. Percec, M. Glodde, T. K. Bera, Y. Miura, I. Shiyanovskaya, K. D. Singer, V. S. K. Balagurusamy, P. A. Heiney, I. Schnell, A. Rapp, H.-W. Spiess S. D. Hudson & H. Duan

Nature **419**, 384–387 (2002).

In this Letter, the volume numbers appeared incorrectly in the footer of pages 384, 385 and 386 as 'VOL 417'. It should have read 'VOL 419'. □

RETRACTION

doi:10.1038/nature14421

Retraction: Histone methylation by the *Drosophila* epigenetic transcriptional regulator Ash1

Christian Beisel, Axel Imhof, Jaime Greene, Elisabeth Kremmer & Frank Sauer

Nature **419,** 857–862 (2002); doi:10.1038/nature01126

The authors and the University of California Riverside wish to retract this Letter owing to inappropriate image manipulation in the published figures. The figure panels affected are Figure 1b, d, Figure 2b, e, Figure 3a and Figure 4d. *Nature* has not received a response from Frank Sauer to approve this retraction.

line (*19*) of 0.1 ng/m^3 by as much as 27-fold on 81% of the mouse exposure days. If PAHs contribute to mutation induction, then the PAH-removal efficiency of our HEPA unit may be an important consideration. Based on chemical analysis of HEPA filters compared to TSP samples from the same location, HEPA filtration blocked 7.1 to 8.0 ng/m^3 (55 to 61%) of total PAHs in ambient air at the urban-industrial site. This is likely to be an underestimate (supporting online text), and HEPA filtration probably removed 55 to 100% of particulate-bound PAHs, substantially reducing exposure for the sentinel mice. PAHs may contribute to germline mutation induction, but we cannot yet make specific conclusions regarding their importance.

Human epidemiological studies have associated air pollution exposure with negative health consequences, including cardiovascular (*20*), respiratory (*21*), and developmental impairments (*22*, *23*) and lung cancer (*1*). Identification of the most dangerous air pollutants and their mode of action in producing specific health effects remains uncertain (*24*). Our study identifies airborne particulate matter as a contributor to heritable mutation induction in mice; however, a direct link between ESTR mutations and health effects has not yet been established. In addition, although elevated germline mutation rates have been documented in both birds (*25*, *26*) and mice (*6*) near industrial areas, it is not clear whether our results can be extrapolated to humans. Nonetheless, structural changes in DNA have been detected in human sperm after air pollution exposure (*27*). Data from mouse studies (*15*, *16*) suggest that a relationship may exist between mutation rates at ESTR loci and those in coding regions of the genome that affect phenotype. To reduce the potential risk of harmful heritable mutations for humans and wildlife, along with a suite of other health problems, we suggest that steps be taken to reduce levels of airborne particulate matter in urban environments.

References and Notes

1. C. A. Pope III *et al.*, *JAMA* **287**, 1132 (2002).
2. D. Palli *et al.*, *Int. J. Cancer* **94**, 121 (2001).
3. S. Burgaz, G. C. Demircigil, B. Karahalil, A. E. Karakaya, *Chemosphere* **47**, 57 (2002).
4. M. Sorensen *et al.*, *Cancer Epidemiol. Biomark. Prevent.* **12**, 191 (2003).
5. S. R. C. Soares *et al.*, *Environ. Res.* **92**, 191 (2003).
6. C. M. Somers, C. L. Yauk, P. A. White, C. L. J. Parfett, J. S. Quinn, *Proc. Natl. Acad. Sci. U.S.A.* **99**, 15904 (2002).
7. H. J. Ettinger, J. D. DeField, D. A. Bevis, R. N. Mitchell, *Am. Ind. Hyg. Assoc. J.* **30**, 20 (1969).
8. Y. Yamada, K. Miyamoto, T. Mori, A. Koizumi, *Health Phys.* **46**, 543 (1984).
9. R. Kelly, G. Bulfield, A. Collick, M. Gibbs, A. J. Jeffreys, *Genomics* **5**, 844 (1989).
10. M. Gibbs, A. Collick, R. Kelly, A. J. Jeffreys, *Genomics* **17**, 121 (1993).
11. P. Bois, J. Williamson, J. Brown, Y. E. Dubrova, A. J. Jeffreys, *Genomics* **49**, 122 (1998).
12. Materials and methods are available as supporting material on *Science* Online.
13. E. Oakberg, *Am. J. Anat.* **99**, 507 (1956).
14. C. Vilarino-Guell, A. G. Smith, Y. E. Dubrova, *Mutat. Res.* **526**, 63 (2003).
15. Y. E. Dubrova *et al.*, *Proc. Natl. Acad. Sci. U.S.A.* **95**, 6251 (1998).
16. Y. E. Dubrova, M. Plumb, *Mutat. Res.* **499**, 143 (2002).
17. Longer times downwind (given a westerly wind direction) of the industrial core area mean more air pollution input from industry and less from the major highway, which is east of the mouse exposure site.
18. A. E. Legzdins, B. E. McCarry, D. W. Bryant, *Polycyclic Aromat. Compd* **5**, 157 (1994).
19. C.-E. Bostrom *et al.*, *Environ. Health Perspect.* **110**, 451 (2002).
20. R. T. Burnett *et al.*, *Am. J. Epidemiol.* **142**, 15 (1995).
21. R. J. Delfino, M. R. Becklake, J. A. Hanley, *Environ. Res.* **67**, 1 (1994).
22. M. Bobak, *Environ. Health Perspect.* **108**, 173 (2000).
23. B. Ritz, F. Yu, G. Fruin, G. M. Shaw, J. A. Harris, *Am. J. Epidemiol.* **155**, 17 (2002).
24. D. Krewski *et al.*, *J. Toxicol. Environ. Health Part A* **66**, 1507 (2003).
25. C. L. Yauk, J. S. Quinn, *Proc. Natl. Acad. Sci. U.S.A.* **93**, 12137 (1996).
26. C. L. Yauk, G. A. Fox, B. E. McCarry, J. S. Quinn, *Mutat. Res.* **452**, 211 (2000).
27. S. G. Selevan *et al.*, *Environ. Health Perspect.* **108**, 887 (2000).

28. We thank K. and G. Gourlay for housing the rural mice on their farm; the Hamilton Port Authority for access to its property; V. Kjoss and S. Kassim for technical support; J. Seaman for flow rate data on the HEPA filtration units; F. Dobroff for weather data from Hamilton Harbour; Y. E. Dubrova, S. Dudley, and an anonymous reviewer for statistical advice; and C. L. Yauk for comments on the manuscript. Supported by the Toxic Substances Research Initiative and the Natural Sciences and Engineering Research Council of Canada.

Supporting Online Material

www.sciencemag.org/cgi/content/full/304/5673/1008/DC1
Materials and Methods
SOM Text
Tables S1 to S4
References and Notes

20 January 2004; accepted 14 April 2004

TAF1 Activates Transcription by Phosphorylation of Serine 33 in Histone H2B

Tobias Maile,[1]* Simona Kwoczynski,[2]*† Rebeccah J. Katzenberger,[3] David A. Wassarman,[3]‡ Frank Sauer[1,2]‡

Dynamic changes in chromatin structure, induced by posttranslational modification of histones, play a fundamental role in regulating eukaryotic transcription. Here we report that histone H2B is phosphorylated at evolutionarily conserved Ser^{33} (H2B-S33) by the carboxyl-terminal kinase domain (CTK) of the *Drosophila* TFIID subunit TAF1. Phosphorylation of H2B-S33 at the promoter of the cell cycle regulatory gene *string* and the segmentation gene *giant* coincides with transcriptional activation. Elimination of TAF1 CTK activity in *Drosophila* cells and embryos reduces transcriptional activation and phosphorylation of H2B-S33. These data reveal that H2B-S33 is a physiological substrate for the TAF1 CTK and that H2B-S33 phosphorylation is essential for transcriptional activation events that promote cell cycle progression and development.

Transcription initiation in eukaryotes involves dynamic changes in chromatin structure that permit assembly of the transcription machinery at a gene promoter (*1*, *2*). The fundamental structural unit of chromatin is the nucleosome, which contains 146 base pairs of DNA wrapped around a histone octamer composed of two copies each of histones H2A, H2B, H3, and H4 (*3*). Distinct patterns of histone modifications (e.g., acetylation, phosphorylation, and methylation) may act as "modification cassettes" that facilitate DNA-dependent events (*4*, *5*). For example, in vertebrates phosphorylation of H2B Ser^{14} is associated with apoptotic chromatin, and in all eukaryotes phosphorylation of H3 Ser^{10} is associated with transcriptionally active and mitotic chromatin (*4*–*6*). Although all histones are phosphorylated in vivo, the function of many of these modifications and the kinases that carry them out are not known (*7*).

With the use of an in vitro kinase assay, we found that the *Drosophila* general transcription factor (GTF) TFIID phosphorylates histone H2B but not H1, H2A, H3, or H4 (Fig. 1, A and B) (*8*). TFIID is a multiprotein complex composed of the TATA box–binding protein (TBP) and numerous TBP-associated factors (TAFs) (*9*). TFIID functions during transcription initiation by nucleating assembly of GTFs and RNA polymerase II at the promoter. TAF1 (formerly TAF$_{II}$250) is the only TFIID subunit that possesses kinase activity, suggesting that it phosphorylates H2B (*10*–*12*). In fact, recombi-

[1]Department of Biochemistry, University of California–Riverside, Riverside, CA 95121, USA. [2]Zentrum für Molekulare Biologie der Universität Heidelberg (ZMBH), Im Neuenheimer Feld 282, 69120 Heidelberg, Germany. [3]Department of Pharmacology, University of Wisconsin (UW)–Madison, 1300 University Avenue, Madison, WI 53706, USA.

*These authors contributed equally to this work.
†Present address: Heidelberger Institut für Pflanzenwissenschaften, Ruprecht-Karls-Universität Heidelberg, Im Neuenheimer Feld 230, 69120 Heidelberg, Germany.
‡To whom correspondence should be addressed. E-mail: frank.sauer@ucr.edu (F.S.), dawassarman@wisc.edu (D.A.W.)

nant TAF1 and denatured and renatured recombinant TAF1 phosphorylated H2B in vitro, demonstrating that TAF1 has intrinsic, H2B-specific kinase activity (Fig. 1, B and C) (*8*). Collectively, these results indicate that TAF1 alone and in the context of TFIID phosphorylates H2B.

TAF1 contains two kinase domains, an N-terminal (NTK, amino acids 1 to 496) and a C-terminal (CTK, amino acids 1496 to 2132) domain (*10*) (Fig. 1D). In vitro, the NTK and the CTK autophosphorylate and the NTK transphosphorylates the RAP74 subunit of the GTF TFIIF. To determine which domain phosphorylates H2B, we assayed NTK and CTK separately in vitro. In contrast to the NTK, the CTK did not phosphorylate RAP74 but strongly phosphorylated H2B, indicating that the CTK possesses H2B-specific kinase activity (Fig. 1E).

Protein kinases contain two essential functional motifs, an adenosine triphosphate (ATP) binding motif and an amino acid–specific kinase motif. Computational sequence comparison analyses identified a putative serine and threonine (S/T) kinase motif (amino acids 1534 to 1546) and two tandem ATP binding domains (amino acids 1747 to 1780) in the CTK (Fig. 2A and fig. S1) (*8*, *13*). To test whether the identified motifs mediate H2B phosphorylation, we performed in vitro kinase assays with the use of CTK polypeptides lacking the S/T kinase motif (CTKΔ1600) or the ATP binding motifs (CTKΔATP). Relative to the wild-type CTK, CTKΔ1600 and CTKΔATP weakly phosphorylated H2B (Fig. 2B and fig. S2A). To confirm the role of the S/T kinase motif, we mutated a catalytically important aspartic acid to an alanine (D1538A) in the motif (Fig. 2A and fig. S1) (*13*). Like CTKΔ1600, CTK(D1538A) exhibited weak autophosphorylation and H2B transphosphorylation activities (Fig. 2B). Interestingly, the S/T kinase motif is located in the first bromodomain of the double bromodomain module (DBD), which binds acetylated lysines (Fig. 2A) (*14*). However, CTK(D1538A) retains the ability to bind acetylated H4 in vitro, indicating that the introduced mutation disrupts kinase activity rather than acetylated lysine-based substrate recognition (fig. S2B). Thus, the identified S/T kinase and ATP binding motifs of the TAF1 CTK are essential for H2B phosphorylation.

To identify H2B residue(s) phosphorylated by the CTK, we first examined whether the CTK phosphorylates the N-terminal tail of *Drosophila* H2B (amino acids 1 to 39, H2BT) or the tailless H2B core domain (amino acids 40 to 123) and found that the CTK phosphorylated H2BT but not the H2B core domain (Fig. 2C). Next, to pinpoint which residue(s) in H2BT is phosphorylated, we generated mutant H2BT peptides in which alanines replaced all or individual serines or threonines. The CTK did not phosphorylate peptides lacking all serines, suggesting that it phosphorylates either Ser^{5} (H2B-S5) or Ser^{33} (H2B-S33) (fig. S2C). To test this, we used H2BT peptides as substrates that contained alanines in place of H2B-S5, H2B-S33, or both (H2BT-S5A, H2BT-S33A, and H2BT-S5/33A, respectively). The CTK phosphorylated H2BT-S5A but not H2BT-S33A or H2BT-S5/33A, indicating that H2B-S33 is the target of the CTK (Fig. 2D).

To investigate whether H2B-S33 is phosphorylated in vivo, we raised a polyclonal antibody recognizing phosphorylated H2B-S33 (H2B-S33P) (*8*). On Western blots, the antibody recognized H2BT containing H2B-S33P but not recombinant, unphosphorylated H2B or an H3 peptide (amino acids 1 to 32) containing phosphorylated Ser^{10} and Ser^{28} (Fig. 3A). In addition, the H2B-S33P antibody recognized H2BT and recombinant H2B that was phosphorylated in vitro by the CTK or TFIID, indicating that the antibody specifically recognizes phosphorylated H2B-S33 (Fig. 3B). The H2B-S33 antibody also recognized a protein with a molecular weight similar to that of H2B from histone preparations from *Drosophila* embryos or S2 cells, providing evidence that H2B-S33 is a target for phosphorylation in vivo (Fig. 3, C and D) (*15*, *16*). To determine whether TAF1 mediates H2B-S33 phosphorylation in vivo, we used RNA interference (RNAi) to eliminate TAF1 expression in S2 cells (*8*). As shown by Western blot analysis, both TAF1 expression and H2B-S33 phosphorylation were reduced in TAF1 RNAi cells compared with mock RNAi cells, suggesting that TAF1 is a major H2B-S33 kinase in vivo (Fig. 3, D and E).

Flow cytometry analysis of TAF1 RNAi cells revealed that loss of TAF1 results in G2-M phase cell cycle arrest (fig. S3). To test the hypothesis that TAF1 controls the transcription of genes whose activities contribute to G2-M progression, we used microarray expression profiling and reverse transcription polymerase chain reaction (RT-PCR) to monitor transcription in mock and TAF1 RNAi cells. Both methods showed that transcription of *string* (*stg*), which encodes a *Drosophila* homolog of yeast Cdc25, was reduced (Fig. 4A) (*8*). The Stg protein phosphatase is predominantly expressed during G2 and activates the cell cycle by dephos-

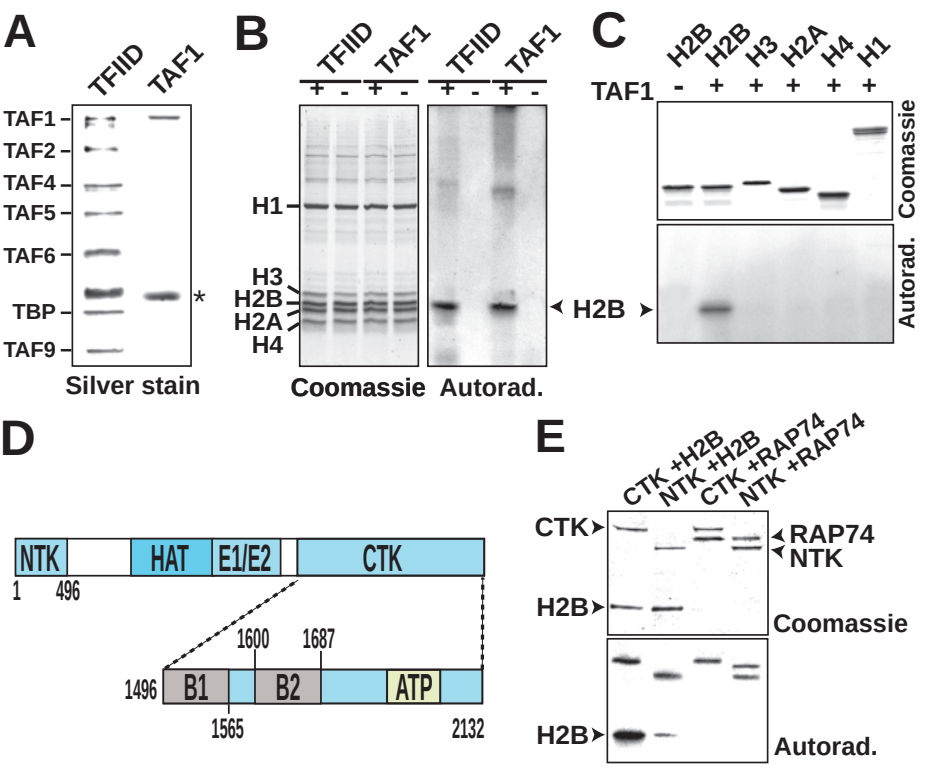

Fig. 1. The TAF1 CTK phosphorylates histone H2B. (**A**) Silver-stained gel of immunopurified TAF1 and endogenous *Drosophila* TFIID. The asterisk indicates the position of the antibody heavy chain. (**B**) Coomassie blue–stained gel (left) and corresponding autoradiogram (right) of in vitro kinase assays programmed with γ^{32}P-ATP and recombinant histones (H1, H2A, H2B, H3, and H4) in the presence (+) or absence (–) of immunopurified TAF1 or TFIID. (**C**) Coomassie blue–stained gel (top) and corresponding autoradiogram (bottom) of in vitro kinase assays as in (B), but containing the indicated recombinant histones and denatured and renatured TAF1. (**D**) Schematic representation of TAF1 and the CTK. Positions of the NTK domain, the HAT domain, the ubiquitin activating and conjugating domain (E1/E2), the DBD (B1 and B2), and the CTK are indicated. (**E**) Coomassie blue–stained gel (top) and corresponding autoradiogram (bottom) of in vitro kinase assays as in (B), except that reactions were programmed with recombinant CTK or NTK and either H2B or RAP74.

phorylating Cdc2 (*17*). Because loss of *stg* from S2 cells by RNAi causes G2-M arrest, TAF1 may regulate G2-M progression by activating *stg* transcription (*18*).

Chromatin immunoprecipitation (XChIP) was used to establish whether there is a direct correlation between transcriptional activation of *stg* and TAF1-mediated phosphorylation of H2B-S33 at the *stg* promoter (*15*). Cross-linked chromatin was isolated from mock and TAF1 RNAi S2 cells and immunoprecipitated with TAF1 or H2B-S33P antibodies. Immunoprecipitated DNA was purified and used as a template for PCR to detect the *stg* promoter or coding region and *actin5C* promoter (Fig. 4B and fig. S4). In contrast, TAF1 is not essential for *actin5C* transcription, and H2B-S33P antibodies do not precipitate the *actin5C* promoter (Fig. 4A and fig. S5A). Thus, the transcriptional dependence of a gene for TAF1 is correlated with H2B-S33 phosphorylation, not with TAF1 association.

To distinguish whether loss of H2B-S33 phosphorylation at the *stg* promoter is due directly to loss of TAF1 or indirectly to G2-M arrest, we performed XChIP analysis on S2 cells arrested in G2-M by RNAi of the SIN3 transcriptional corepressor. *Stg* transcription is repressed in SIN3 RNAi cells, yet the *stg* promoter remains associated with H2B-S33P and TAF1, indicating that loss of H2B-S33 phosphorylation in TAF1 RNAi cells is because of elimination of TAF1 rather than G2-M arrest (fig. S5B) (*18*).

In addition to kinase domains, TAF1 has a histone acetyltransferase (HAT) domain that acetylates H3 Lys^{14} (H3-K14) and unidentified lysines in H4 in vitro (*19*). XChIP analysis detected acetylated H3-K14 and H4 at the transcriptionally active *stg* promoter in mock RNAi cells but not at the inactive *stg* promoter in TAF1 RNAi cells (Fig. 4B and fig. S5C). In contrast, TAF1-independent histone modifications did not correlate with activation of *stg* in mock and TAF1 RNAi cells (fig. S5C). Taken together, these results indicate that TAF1-mediated phosphorylation of H2B-S33 and acetylation of H3 and H4 potentiate transcriptional activation in *Drosophila* cells.

To investigate the role of TAF1-mediated phophorylation of H2B-S33 during fly development, we used a recessive lethal *TAF1* allele, $TAF1^{CTK}$, which contains a nonsense mutation at amino acid 1728 that truncates the CTK downstream of the DBD (Fig. 2A and fig. S6A) (*8*). The corresponding protein (TAF1ΔCTK) is expressed in *Drosophila* but presumably does not have CTK activity, because it does not phosphorylate H2B in vitro (Fig. 2B and fig. S6, B and C). In situ hybridization was used to monitor transcription in embryos homozygous mutant for $TAF1^{CTK}$ and heterozygous mutant for the maternal activator Caudal (Cad) (*20*). In this genetic background, transcription of the gap gene *giant* (*gt*) was reduced (Fig. 4C). *Gt* is transcribed in two domains along the anterior-posterior axis of blastoderm-stage embryos. Transcription of the posterior *gt* domain (pgt) is Cad-dependent, whereas transcription of the anterior *gt* domain (agt) is Cad-independent. Relative to controls (*cad*/+ or $TAF1^{CTK}$), pgt transcription was reduced in *cad*/+;$TAF1^{CTK}$ embryos (Fig. 4C).

XChIP analysis was used to examine whether TAF1-mediated phosphorylation of H2B-S33 contributes to pgt transcription. Cross-linked chromatin was isolated from the posterior halves of *cad*/+;$TAF1^{CTK}$ and control embryos and immunoprecipitated with antibodies to H2B-S33P, acetylated histones, or TAF1. PCR analysis detected H2B-S33P at the transcriptionally active *gt* promoter in control embryos, but not at the transcriptionally repressed promoter in *cad*/+;$TAF1^{CTK}$ embryos (Fig. 4D and fig. S4). To monitor TAF1 binding, we used two antibodies, TAF1-M and TAF1-C, which recognize the middle domain and the CTK of TAF1, respectively (fig. S6A). Both antibodies precipitated the *gt* promoter from control embryos, indicating that TAF1ΔCTK and maternally contributed, wild-type TAF1 are present at the *gt* promoter in the pgt (Fig. 4D and fig. S4). In contrast, although the TAF1-M antibody precipitated the *gt* promoter from *cad*/+;$TAF1^{CTK}$ embryos, TAF1-C did not. Because TAF1ΔCTK is present at a higher concentration in *cad*/+;$TAF1^{CTK}$ embryos than maternal TAF1, this result indicates that TAF1ΔCTK is preferentially recruited to the *gt* promoter in the pgt (Fig. 4D and fig. S6C). This result is supported by the presence of TAF1-mediated histone acetylation at the transcriptionally silent *gt* promoter. Thus, TAF1-mediated phosphorylation of H2B-S33 contributes to transcriptional activation during *Drosophila* embryogenesis.

Ser^{33} is the only evolutionarily conserved serine or threonine in the N-terminus of metazoan H2Bs (fig. S7). In the crystal structure of the *Xenopus laevis* nucleosome, the equiv-

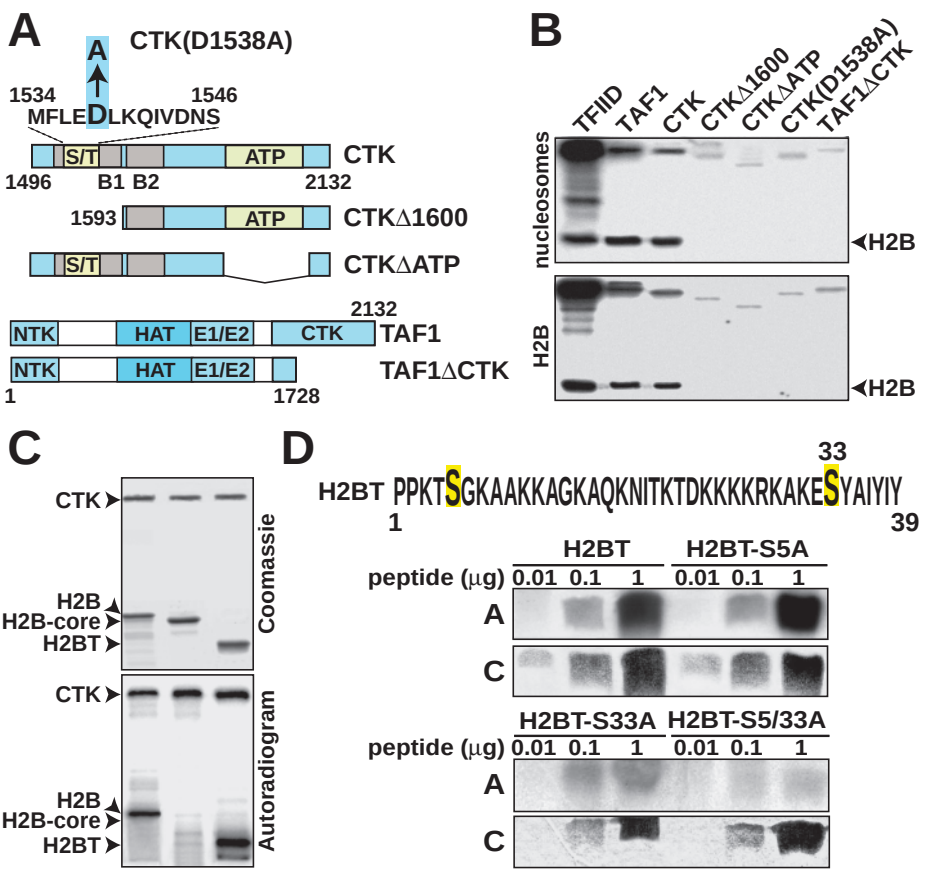

Fig. 2. The TAF1 CTK phosphorylates Ser^{33} in H2B. (**A**) Schematic representation of TAF1 and TAF1 derivatives. The positions of enzymatic domains are indicated. The position and amino acid sequence (*30*) of the S/T kinase motif and the positions of the ATP-binding motifs and CTK(D1538A) mutation are indicated. (**B**) Autoradiograms of in vitro kinase assays containing γ^{32}P-ATP, native nucleosomes (top) or recombinant H2B (bottom), and TFIID, TAF1, or TAF1 derivatives. (**C**) Coomassie blue–stained gel (top) and corresponding autoradiogram (bottom) of in vitro kinase assays programmed with γ^{32}P-ATP, CTK, and H2B, tailless H2B core domain (H2B-core), or H2BT peptide. (**D**) Schematic representation of H2BT (top). Serines (S) are highlighted. Autoradiograms (A) and corresponding Coomassie blue–stained gels (C) of in vitro kinase assays containing TAF1, γ^{32}P-ATP, and increasing amounts of H2BT or H2BT derivatives (bottom).

alent serine links the H2B DNA-binding N-terminal tail to the histone fold domain (*3*, *21*). Thus, replacing the hydroxyl group on Ser^{33} with a bulkier, negatively charged phosphate group may drastically affect H2B tail interactions with DNA. This is important because the H2B tail regulates nucleosome mobility. Deletion of the tail bypasses the requirement for the SWI/SNF nucleosome-remodeling complex in yeast, and the tail is critical for maintaining the position of histone octamers in in vitro sliding assays (*22*, *23*). These findings support a model in which TAF1-mediated phosphorylation of H2B-S33 disrupts DNA-histone interactions, resulting in local decondensation of chromatin. Decondensation may trigger chromatin remodeling and formation of a chromatin structure that facilitates assembly of other GTFs at a promoter, a function that is primarily attributed to TFIID (*1*, *2*, *10*).

Our data indicates that the S/T kinase motif of the CTK is located in the DBD. In the crystal structure of the DBD, the position of the S/T kinase motif does not overlap with the acetylated lysine-binding surface of the DBD, suggesting that it is an independent functional unit of the DBD (*14*). Members of the *fsh*/RING3 (BET) family of DBD proteins have kinase activity, suggesting that TAF1 is a member of a kinase family whose catalytic motif resides within the DBD (*24*, *25*).

Phosphorylation of H2B-S33 by TAF1 is essential for transcriptional activation of *stg*/*cdc25* and, consequently, cell cycle progression. Similarly, depletion of yeast TAF5, human TAF2, or a twofold reduction in chicken TBP results in G2-M arrest (*26*–*28*). Like TAF1, TBP regulates *stg*/*cdc25* expression, providing support for the finding that the H2B-S33 kinase activity of TAF1 occurs in the context of TFIID (*28*). Interestingly, depletion of yeast TAF1, which does not possess a CTK, and inactivation of TAF1 HAT activity induce G1 arrest because of reduced transcription of B- and D-type cyclins, respectively (*26*, *29*). Thus, loss of all TAF1 activities causes G2-M arrest whereas loss of TAF1 HAT activity causes G1 arrest, suggesting gene-specific requirements for TAF1 CTK and HAT activities. In contrast, the presence of phosphorylated H2B-S33 and acetylated H3 and H4 at the *stg* and *gt* promoters implies that TAF1 CTK and HAT activities can cooperate in transcriptional activation of some genes. This proposal is supported by the finding that loss of H2B-S33P from the *gt* promoter results in reduced transcription, despite the presence of TAF1-mediated histone acetylation. Thus, TAF1-mediated phosphorylation of H2B-S33 may work in concert with other TAF1-mediated histone modifications, H1 ubiquitination, and H3 and H4 acetylation to contribute to the chromatin-based mechanisms underlying transcription activation of eukaryotic genes.

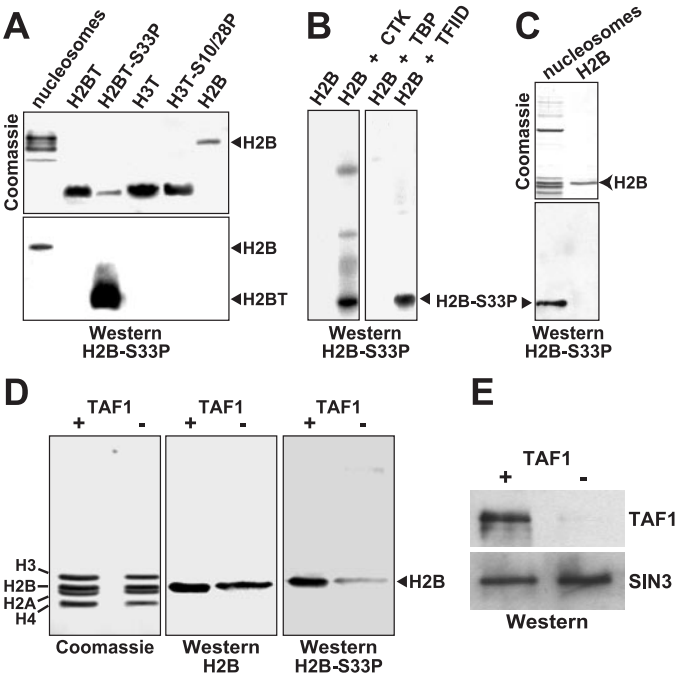

Fig. 3. H2B Ser^{33} is phosphorylated in *Drosophila*. (**A**) Coomassie blue–stained gel (top) and corresponding Western blot (bottom) of purified nucleosomes, H2BT, H2BT-S33P peptide (phosphorylated at Ser^{33}), H3T peptide, H3T-S10/28P peptide (phosphorylated at Ser^{10} and Ser^{28}), and recombinant H2B. Phosphorylation of H2B-S33 was monitored with the H2B-S33P antibody. (**B**) Western blots of in vitro kinase assays programmed with ATP, recombinant H2B, and TAF1 CTK, TBP, or TFIID and probed with the H2B-S33P antibody. (**C**) Coomassie blue–stained gel (top) and corresponding Western blot (bottom) of nucleosomal histones purified from embryos and recombinant H2B and probed with the H2B-S33P antibody. (**D**) Coomassie blue–stained gel (left) and corresponding Western blots (middle and right) of histone octamers purified from mock (+) or TAF1 (–) RNAi S2 cells. The same Western blot was probed with the H2B-S33P antibody, stripped, and reprobed with an H2B antibody as a loading control. (**E**) Western blots of whole cell extracts from mock (+) or TAF1 (–) RNAi S2 cells probed with antibodies to TAF1 (top) or SIN3 (bottom).

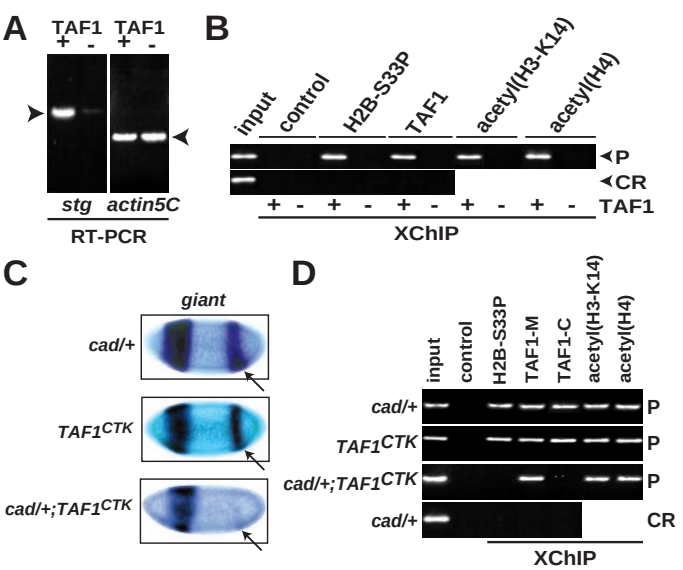

Fig. 4. Transcription activation in *Drosophila* coincides with TAF1-mediated phosphorylation of H2B-S33. (**A**) Photographs of ethidium bromide–stained agarose gels showing RT-PCR products for *stg* (left) and *actin5C* (right) transcripts in mock (+) and TAF1 (–) RNAi S2 cells. (**B**) Photographs of ethidium bromide–stained agarose gels showing PCR products for the *stg* promoter (P) or coding region (CR) in mock (+) and TAF1 (–) RNAi S2 cells. In vivo cross-linked chromatin was immunoprecipitated with the indicated antibodies or rabbit preimmune serum (control). Input represents the amount of *stg* promoter present in 0.1% of the chromatin used for XChIP. (**C**) *Gt* transcription in heterozygous mutant *cad* (top), homozygous mutant $TAF1^{CTK}$ (middle), or heterozygous mutant *cad* and homozygous mutant $TAF1^{CTK}$ (bottom) blastoderm-stage *Drosophila* embryos. *Gt* transcription was detected by in situ hybridization with *gt* anti-sense RNA. Anterior is to the left and dorsal is up. Arrows indicate the position of the posterior *gt* transcription domain. (**D**) Photographs of ethidium bromide–stained agarose gels showing PCR products for the *gt* promoter (P) or coding region (CR) in embryos described in (C). In vivo cross-linked chromatin was isolated from the posterior halves of embryos and immunoprecipitated with the indicated antibodies or rabbit preimmune serum (control). Input represents the amount of *gt* promoter present in 2% of the chromatin used for XChIP.

References and Notes

1. B. Lemon, R. Tjian, *Genes Dev.* **14**, 2551 (2000).
2. G. Orphanides, D. Reinberg, *Cell* **108**, 439 (2002).
3. K. Luger, A. W. Mader, R. Richmond, D. F. Sargent, T. J. Richmond, *Nature* **389**, 251 (1997).
4. M. G. Goll, T. H. Bestor, *Genes Dev.* **16**, 1739 (2002).

5. W. Fischle, Y. Wang, C. D. Allis, *Nature* **425**, 475 (2003).
6. W. L. Cheung *et al*., *Cell* **113**, 507 (2003).
7. I. Isenberg, *Annu. Rev. Biochem.* **48**, 159 (1979).
8. Materials and methods are available as supporting material on *Science* Online.
9. B. S. Chen, M. Hampsey, *Curr. Biol.* **12**, R620 (2002).
10. R. Dikstein, S. Ruppert, R. Tjian, *Cell* **84**, 781 (1996).
11. D. A. Wassarman, F. Sauer, *J. Cell Sci.* **114**, 2895 (2001).
12. A.-D. Pham, F. Sauer, *Science* **289**, 2357 (2000).
13. S. C. Elgin, J. Schilling, L. E. Hood, *Biochemistry* **18**, 5679 (1979).
14. R. H. Jacobson, A. G. Ladurner, D. S. King, R. Tjian, *Science* **288**, 1422 (2000).
15. C. Beisel, A. Imhof, J. Greene, E. Kremmer, F. Sauer, *Nature* **419**, 857 (2002).
16. P. T. Georgel, T. Tsukiyama, C. Wu, *EMBO J.* **16**, 4717 (1997).
17. M. S. Lee *et al*., *Mol. Biol. Cell* **3**, 73 (1992).
18. L. A. Pile, E. M. Schlag, D. A. Wassarman, *Mol. Cell. Biol.* **22**, 4965 (2002).
19. C. A. Mizzen *et al*., *Cell* **87**, 1261 (1996).
20. R. Rivera-Pomar, H. Jäckle, *Trends Genet.* **12**, 478 (1996).
21. K. Luger, T. J. Richmond, *Curr. Opin. Struct. Biol.* **8**, 33 (1998).
22. J. Recht, M. A. Osley, *EMBO J.* **18**, 229 (1999).
23. A. Hamiche, J.-G. Kang, C. Dennis, H. Xiao, C. Wu, *Proc. Natl. Acad. Sci. U.S.A.* **98**, 14316 (2001).
24. L. Zheng, M. M. Zhou, *FEBS Lett.* **513**, 124 (2002).
25. B. Florence, D. V. Faller, *Front. Biosci.* **6**, D1008 (2001).
26. L. M. Apone, C. M. Verasius, J. C. Reese, M. R. Green, *Genes Dev.* **10**, 2368 (1996).
27. J. Martin, R. Halenbeck, J. Kaufmann, *Mol. Cell. Biol.* **19**, 5548 (1999).
28. M. Um, J. Yamauchi, S. Kato, J. L. Manley, *Mol. Cell. Biol.* **21**, 2435 (2002).
29. E. L. Dunphy, T. Johnson, S. S. Auerbach, E. H. Wang, *Mol. Cell. Biol.* **20**, 1134 (2001).
30. Single-letter abbreviations for the amino acid residues are as follows: A, Ala; C, Cys; D, Asp; E, Glu; F, Phe; G, Gly; H, His; I, Ile; K, Lys; L, Leu; M, Met; N, Asn; P, Pro; Q, Gln; R, Arg; S, Ser; T, Thr; V, Val; W, Trp; and Y, Tyr.

31. We thank S. Hansen and R. Tjian for the RAP74 expression plasmid, K. Schell and J. Batchelder at the UW-Madison Comprehensive Cancer Flow Cytometry Facility for their assistance, and C. Metcalf and T. Sanchez-Elsner for comments that improved the manuscript. This work was supported by an NIH grant (GM066204-02) to D.A.W. and a Volkswagen Stiftung grant (I/77 996) to F.S.

Supporting Online Material

www.sciencemag.org/cgi/content/full/304/5673/1010/DC1
Materials and Methods
Figs. S1 to S7
References and Notes

22 December 2003; accepted 6 April 2004

Regulation of Phagosome Maturation by Signals from Toll-Like Receptors

J. Magarian Blander and Ruslan Medzhitov*

In higher metazoans, phagocytosis is essential in host defense against microbial pathogens and in clearance of apoptotic cells. Both microbial and apoptotic cells are delivered on a common route from phagosomes to lysosomes for degradation. Here, we found that activation of the Toll-like receptor (TLR) signaling pathway by bacteria, but not apoptotic cells, regulated phagocytosis at multiple steps including internalization and phagosome maturation. Phagocytosis of bacteria was impaired in the absence of TLR signaling. Two modes of phagosome maturation were observed, constitutive and inducible; their differential engagement depended on the ability of the cargo to trigger TLR signaling.

Phagocytosis is an ancient form of host defense (*1*) performed by specialized phagocytes, such as macrophages (*2*–*6*). Although the phagocytosis of bacteria and apoptotic cells relies on the same cellular machinery (*7*), the immunological response differs (*4*–*6*), as determined primarily by the engagement of TLRs (*6*, *8*).

To examine whether TLR signaling regulates phagocytosis, we compared macrophages from wild-type (WT), MyD88$^{-/-}$, and TLR2x4$^{-/-}$ mice (generated from TLR2$^{-/-}$ × TLR4$^{-/-}$ mice crossed to homozygosity). Phagocytosis was performed in serum-free media to eliminate contributions of Fc and/or complement receptors (*6*, *9*). MyD88$^{-/-}$ and TLR2x4$^{-/-}$ macrophages were unresponsive to inactivated *Escherichia coli* (fig. S1). Fluorescent bacteria were used to monitor phagocytosis in a time- and dose-dependent manner by a fluorescence activated cell sorter (FACS) assay (*10*) (fig. S2). MyD88$^{-/-}$ and TLR2x4$^{-/-}$ macrophages internalized recombinant green fluorescent protein (GFP)–expressing *E. coli* at reduced

Howard Hughes Medical Institute, Section of Immunobiology, Yale University School of Medicine, New Haven, Connecticut 06520, USA.

*To whom correspondence should be addressed. E-mail: ruslan.medzhitov@yale.edu

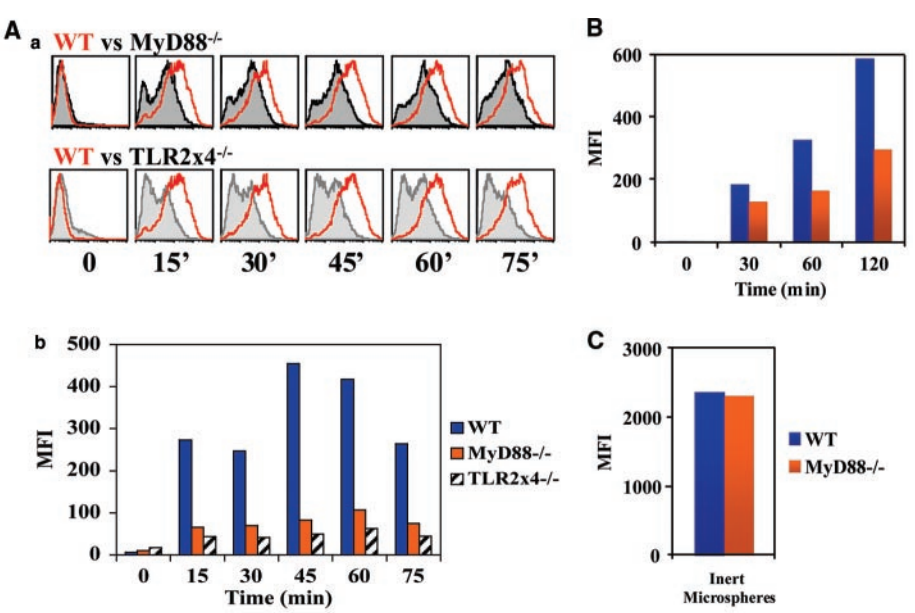

Fig. 1. Impaired phagocytosis in the absence of a TLR-MyD88 signal. Bone marrow (BM)–derived macrophages given *E. coli*–GFP at a ratio of 1:100. (**A**) (a) FACS histograms representative of at least 10 experiments and showing phagocytosis in serum-free conditions by WT (red), MyD88$^{-/-}$ (tinted, top panels), or TLR2x4$^{-/-}$ BM-derived macrophages (tinted, bottom panels) at 37°C. GFP fluorescence is plotted on the *x* axis, on a logarithmic scale ranging from 10^0 to 10^4, and cell number is plotted on the *y* axis. (b) Mean fluorescence intensities (MFIs) of GFP from (a). (**B**) MFIs showing phagocytosis of serum-opsonized *E. coli*–GFP by WT or MyD88$^{-/-}$ macrophages at various times in the presence of serum [similar results in TLR4$^{-/-}$ macrophages (*11*)]. Plot legend is as in (C). (**C**) MFIs at 2 hours after phagocytosis of FluoSpheres under serum-free conditions by WT or MyD88$^{-/-}$ macrophages, as indicated in the legend.

RETRACTION

Post date 30 May 2014

Science has received the results of the University of California, Riverside Committee on Privilege and Tenure's investigation of the papers published in *Science* by Professor Frank Sauer and colleagues, "TAF1 activates transcription by phosphorylation of serine 33 in histone H2B" (*1*) and "Noncoding RNAs of trithorax response elements recruit *Drosophila* Ash1 to Ultrabithorax" (*2*).

For the 2004 Report (*1*), the Committee's findings can be summarized as follows: Lanes 3 and 4 in Fig. 1B were replicated from a figure in another paper (*3*). There was manipulation of gel images that constituted data falsification and fabrication in Fig. 2C; Fig. 3, B and C; Fig. 4, B and D; and panel A in fig. S5C.

For the 2006 Research Article (*2*), the Committee's findings can be summarized as follows: In Fig 6C, there was replication of the same image in two panels that constitutes data falsification. There was manipulation of gel images that constituted data falsification and fabrication in Fig. 4D; Fig. 6, A and B; and fig. S5A.

The Committee concluded that the image manipulations described above constituted a significant departure from the accepted practices of Dr. Sauer's research community. Therefore, the data, results, and conclusions in the papers are clearly not reliable. *Science* is hereby retracting the papers, at the request of University of California, Riverside and Dr. Sauer. The Committee determined that Dr. Sauer was the sole individual responsible for producing the figures.

– MARCIA MCNUTT
Editor-in-Chief

References

1. T. Maile, S. Kwoczynski, R. J. Katzenberger, D. A. Wassarman, F. Sauer, *Science* **304**, 1010 (2004).
2. T. Sanchez-Elsner, D. Gou, E. Kremmer, F. Sauer, *Science* **311**, 1118 (2006).
3. C. Beisel, A. Imhof, J. Greene, E. Kremmer, F. Sauer, *Nature* **419**, 857 (2002).

TAF1 Activates Transcription by Phosphorylation of Serine 33 in Histone H2B

Tobias Maile *et al.*

Science **304**, 1010 (2004);
DOI: 10.1126/science.1095001

RETRACTED 30 MAY 2014; SEE LAST PAGE

Noncoding RNAs of Trithorax Response Elements Recruit *Drosophila* Ash1 to Ultrabithorax

Tilman Sanchez-Elsner,[1] Dawei Gou,[1] Elisabeth Kremmer,[2] Frank Sauer[1]*

Homeotic genes contain cis-regulatory trithorax response elements (TREs) that are targeted by epigenetic activators and transcribed in a tissue-specific manner. We show that the transcripts of three TREs located in the *Drosophila* homeotic gene *Ultrabithorax* (*Ubx*) mediate transcription activation by recruiting the epigenetic regulator Ash1 to the template TREs. TRE transcription coincides with *Ubx* transcription and recruitment of Ash1 to TREs in *Drosophila*. The SET domain of Ash1 binds all three TRE transcripts, with each TRE transcript hybridizing with and recruiting Ash1 only to the corresponding TRE in chromatin. Transgenic transcription of TRE transcripts restores recruitment of Ash1 to *Ubx* TREs and restores *Ubx* expression in *Drosophila* cells and tissues that lack endogenous TRE transcripts. Small interfering RNA–induced degradation of TRE transcripts attenuates Ash1 recruitment to TREs and *Ubx* expression, which suggests that noncoding TRE transcripts play an important role in epigenetic activation of gene expression.

The identity of cells in metazoan organisms is established during development and mitotically propagated throughout the entire life cycle. Phylogenetically highly conserved protein families of epigenetic regulators determine the fate of developing cells by establishing and maintaining mitotically stable gene expression programs (*1*–*4*). In *Drosophila*, members of the trithorax group (trxG) of epigenetic regulators maintain active transcription states, whereas members of the Polycomb group (PcG) maintain repressed transcription states (*2*–*4*). Many epigenetic regulators control gene expression by establishing transcriptional competent or silent chromatin structures (*5*, *6*). Several epigenetic activators [Trx, trithorax-related (Trr)] and repressors (Enhancer of zeste) are lysine-specific histone methyltransferases (HMTs) and contain a SET domain, the catalytic hallmark motif of HMTs. Methylation of lysine residues in histones H3 and H4 has been correlated with epigenetic activation [Lys^4 in H3 (H3-K4)] and repression [Lys^9 and Lys^{27} in H3 (H3-K9)] (*6*–*8*).

We previously showed that the epigenetic activator "absent small and homeotic discs" (Ash1) promotes transcriptional activation by trimethylating H3-K4, H3-K9, and Lys^{20} in H4 (H4-K20) (*9*). Ash1 maintains activated transcription states in larval imaginal discs that give rise to the appendages in the adult fly (*10*, *11*). For example, Ash1 is essential for the expression of the homeotic gene *Ultrabithorax* (*Ubx*) in third-leg and haltere imaginal discs, and *Ubx* expression coincides with Ash1-mediated histone methylation (*9*–*11*).

PcG and trxG regulators are recruited to specific chromosomal elements that are present in the cis-regulatory region of target genes (*2*–*4*). The same element can act as an activating or a silencing module (*4*). In the repressed state, the elements represent Polycomb response elements (PREs) and facilitate the recruitment of PcG proteins (*2*–*4*). In the activated state, the DNA-elements function as trithorax response elements (TREs) and recruit trxG proteins (*3*, *4*). Transcription of noncoding RNAs (ncRNAs) from TRE/PRE elements switches silent PREs into TREs, which indicates that TRE/PRE transcription plays an important role in epigenetic activation (*12*–*15*). How transcription of TREs culminates in the recruitment of trxG regulators is unknown. Here, we address the question of how epigenetic regulators without known DNA binding capabilities, such as Ash1 (*16*), recognize and bind target genes in chromatin.

***Ubx* TREs are transcribed in *Drosophila* imaginal discs.** The coincidence of the tissue-specific transcription and trans-regulatory activity patterns of TREs and trxG proteins, respectively, suggests that not only TRE/PRE transcription but also the resulting ncRNAs might play a role in epigenetic activation (*12*–*15*). Here, we analyze the role of ncRNAs transcribed from three *Ubx* TRE/PREs. The *Ubx* locus contains a cluster of three characterized TRE/PREs (TRE1 to TRE3) within the boundaries of the chromosomal memory element (CME) *bxd* that is located 22 kb upstream of the *Ubx* promoter (Fig. 1A) (*17*, *18*).

To correlate the transcriptional activity of *Ubx* with *bxd* transcription in *Drosophila*, we used rapid amplification of cDNA ends (RACE) to detect *bxd* transcripts in third-leg discs. Three capped, polyadenylated *bxd* transcripts transcribed by RNA polymerase II were detected in third-leg and haltere discs (*tre1*, *tre2*, *tre3*) (Fig. 1A) (*19*).

We next used the reverse transcription polymerase chain reaction (RT-PCR) to determine

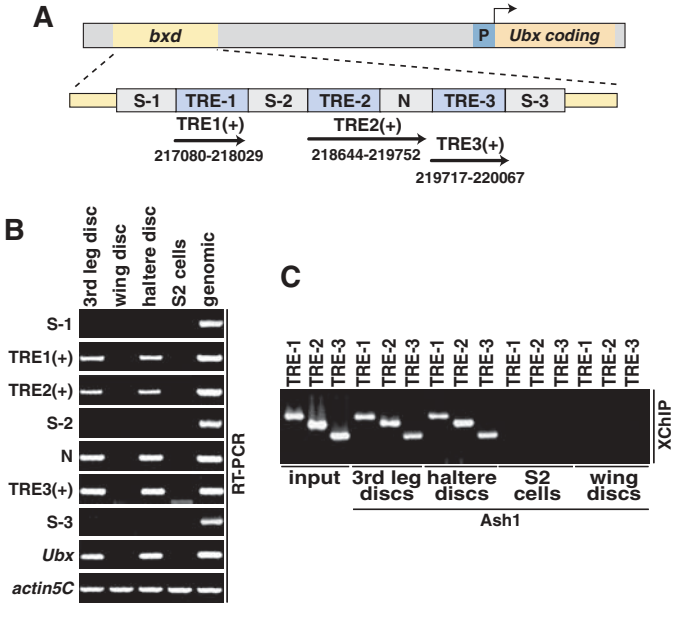

Fig. 1. Cell type–specific transcription of *Ubx* TREs. (**A**) Schematic representation of the *Ubx* locus (top) and the *bxd* DNA element (bottom). The positions of *bxd*, *Ubx* promoter (P), TREs, spacer DNA (S-1, S-2, N, and S-3) are indicated. The orientation and position (*22*) of TRE transcripts in *bxd* are indicated. (**B**) RT-PCR assays were used to detect the transcripts of the indicated *bxd* elements and control transcripts (*actin5C*, *Ubx*) in imaginal discs (third-leg, haltere, and wing), Schneider S2 cells, and genomic DNA. (**C**) PCR analysis of XChIP immunoprecipitates detecting the association of Ash1 with *Ubx* TREs in imaginal discs and S2 cells. Input represents the amount of transcripts or TREs detected in 0.5% of the starting material.

[1]Department of Biochemistry, University of California, Riverside, CA 92521, USA. [2]Institut für Molekulare Immunologie, GSF-Forschungszentrum für Umwelt und Gesundheit, Marchioninistr. 25, 81377 München, Germany.

*To whom correspondence should be addressed: E-mail: frank.sauer@ucr.edu

whether the presence of the three TRE transcripts coincides with *Ubx* transcription. RNA was isolated from third-leg discs and haltere imaginal discs (haltere discs), which both transcribe *Ubx*, and from wing imaginal discs (wing discs) and embryonic *Drosophila* Schneider 2 (S2) cells that do not transcribe *Ubx* (*9*–*11*). Transcripts from *Ubx* and all three TREs were detected in third-leg and haltere discs, whereas *Ubx* and TRE transcripts were not detected in S2 cells and wing discs (Fig. 1B) (figs. S1 and S2).

Recruitment of Ash1 to *Ubx* TREs. To investigate whether Ash1 is recruited to transcriptionally active *Ubx* TREs, we used in vivo cross-linked chromatin immunoprecipitation (XChIP) to detect Ash1 at the *Ubx* TREs in third-leg, haltere, and wing discs and in S2 cells, all of which express *ash1* (*9*, *10*). Ash1 was detected at all three TREs in third-leg and haltere discs (Fig. 1C). In addition, the characteristic Ash1 histone methylation pattern was detectable in all three TREs and the transcriptionally active *Ubx* promoter in third-leg discs (Fig. 1C and Fig. 2A). Ash1 was not detected at the TREs of the transcriptionally inactive *Ubx* locus in wing discs and S2 cells, which do not transcribe TREs (Fig. 1C).

We also compared the recruitment of Ash1 to *Ubx* in wild-type and homozygous mutant $ash1^{22}$ third-leg discs by XChIP. The $ash1^{22}$ mutant is recessive lethal and expresses a truncated protein that lacks the SET domain and trans-activation activity (*10*). Ash1 and the characteristic Ash1 histone methylation pattern were detected at the transcriptionally active *Ubx* locus in wild-type discs but not in $ash1^{22}$ mutant discs (Fig. 2, A and B) (fig. S3); this finding indicates that recruitment of Ash1 and Ash1-mediated histone methylation coincides with activation of *Ubx* expression in third-leg discs. We monitored TRE transcription in the wild-type and $ash1^{22}$ mutant third-leg discs by RT-PCR. TRE transcripts were detected at comparable levels in wild-type and mutant discs, which indicates that Ash1 is not a major regulator of TRE transcription in imaginal discs (Fig. 2C) (fig. S3).

Ash1 SET domain interacts with TRE transcripts in vitro. The association of Ash1 with TREs in cells producing TRE transcripts suggests that TRE transcription or TRE transcripts nucleate recruitment of Ash1 to *Ubx* TREs. SET-domain proteins can bind single-stranded RNA and DNA in vitro, and ncRNA has been implicated in protein recruitment in gene dosage compensation (*20*–*24*). We used in vitro protein-RNA binding assays to assess whether Ash1 associates with TRE transcripts. Ash1SET, which consists of amino acids 1001 to 1619, retained TRE1(+), TRE2(+), and TRE3(+) but not the H3-K9–specific HMT Medusa (Mdu) (Fig. 3A) (fig. S4). In contrast, Ash1, Ash1ΔN, and Mdu did not bind the antisense RNA of the *Ubx* TREs (Fig. 3A) (fig. S4). Ash1ΔN did not interact with the N-element in *tre2* (Fig. 3A), which corresponds to the DNA spacer separating TRE-2 and TRE-3 (Fig. 1A).

In competition experiments, unlabeled TRE transcripts could outcompete the interaction of Ash1 with the corresponding TRE transcript (fig. S5). In contrast, double-stranded TRE transcripts, double-stranded DNA TRE sequences, and DNA-RNA hybrids consisting of TRE transcripts and TREs failed to disrupt the interaction; these findings suggest that Ash1 associates with single-stranded TRE transcripts (fig. S5).

To delineate the RNA-binding motif of Ash1, we investigated the interaction of truncated *ash1* proteins with TRE transcripts. In addition to Ash1SET, we tested Ash1ΔN (amino acids 1001 to 2218), which contains the Ash1 SET module, and Ash1N (amino acids 1 to 1001) and Ash1C (amino acids 1619 to 2218), which both lack the SET domain and cysteine-rich regions (Fig. 3B). Ash1ΔN and Ash1SET, but not Ash1N and Ash1C, retained TRE transcripts, indicating that the SET domain of Ash1 binds TRE transcripts in vitro (Fig. 3C).

RNA-dependent recruitment of Ash1 to *Ubx* TREs in *Drosophila*. We next used XChIP to investigate whether Ash1 associates with TRE transcripts in vivo. Ash1 coprecipitated with TRE transcripts but not control transcripts from mock-treated chromatin (Fig. 3D) (fig. S6). Ash1 bound TRE transcripts in ribonuclease (RNase) III–treated chromatin, indicating that double-stranded RNA (dsRNA) motifs within TRE transcripts do not mediate the association of TRE transcripts with Ash1 in vivo (Fig. 3D) (fig. S7). In contrast, Ash1 did not interact with TRE transcripts from RNase A– and RNase H–treated chromatin, indicating that single-stranded RNA (ssRNA) is important for the association of Ash1 with TRE transcripts (Fig. 3D) (fig. S7). The disruption of the association between Ash1 and TRE transcripts by RNase H (which degrades DNA-RNA hybrids) in chromatin suggests that TRE transcripts hybridize with DNA in chromatin.

Is the association of Ash1 with TREs dependent on RNA? We used XChIP to compare the interaction of Ash1 and TRE in mock- and RNase-treated chromatin. Antibodies to Ash1 precipitated all three TREs, but not the spacer DNAs (S-2), from mock-treated and RNase III–treated chromatin, indicating that dsRNA does not contribute to the interaction of Ash1 with TREs (Fig. 3E) (fig. S7). In contrast, treating chromatin with RNase H or RNase A attenuated the association of Ash1 with TREs, indicating that the association of Ash1 with the *Ubx* TREs is RNA-dependent (Fig. 3E) (fig. S7). The disruption of the interaction of Ash1 with TREs in chromatin by RNase H and RNase A raises the possibility that ssRNA motifs in RNA-DNA hybrids play a role in the recruitment of Ash1 to TREs.

To verify that the observed attenuation of Ash1-TRE interactions is based on specific rather than general disruption of protein-DNA interactions in RNase-treated chromatin, we investigated the recruitment of the general transcription factor TFIID to target genes in mock- and RNase-treated chromatin (*25*). The TATA-binding protein (TBP) subunit of TFIID

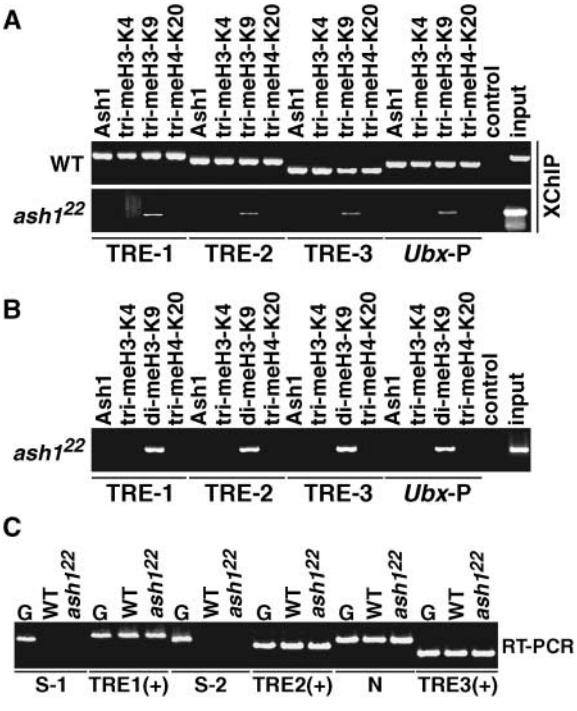

Fig. 2. Recruitment of Ash1 to *Ubx* TREs in third-leg imaginal discs. (**A**) PCR analysis of XChIP immunoprecipitates detecting the association of Ash1 and the Ash1 histone methylation pattern at the TREs and promoter of *Ubx* in wild-type (WT) and $ash1^{22}$ mutant third-leg imaginal discs. In vivo cross-linked chromatin was immunoprecipitated with the indicated antibodies and rat/rabbit antiserum (control). Input represents the amount of TRE-1 detected in 0.5% of the starting material. (**B**) XChIP analysis as described in (A), except that chromatin was immunoprecipitated with an antibody to di-methylated H3-K9. (**C**) RT-PCR analysis detecting *bxd* transcripts in RNA pools isolated from wild-type (WT) and $ash1^{22}$ mutant third-leg discs or in genomic DNA (G).

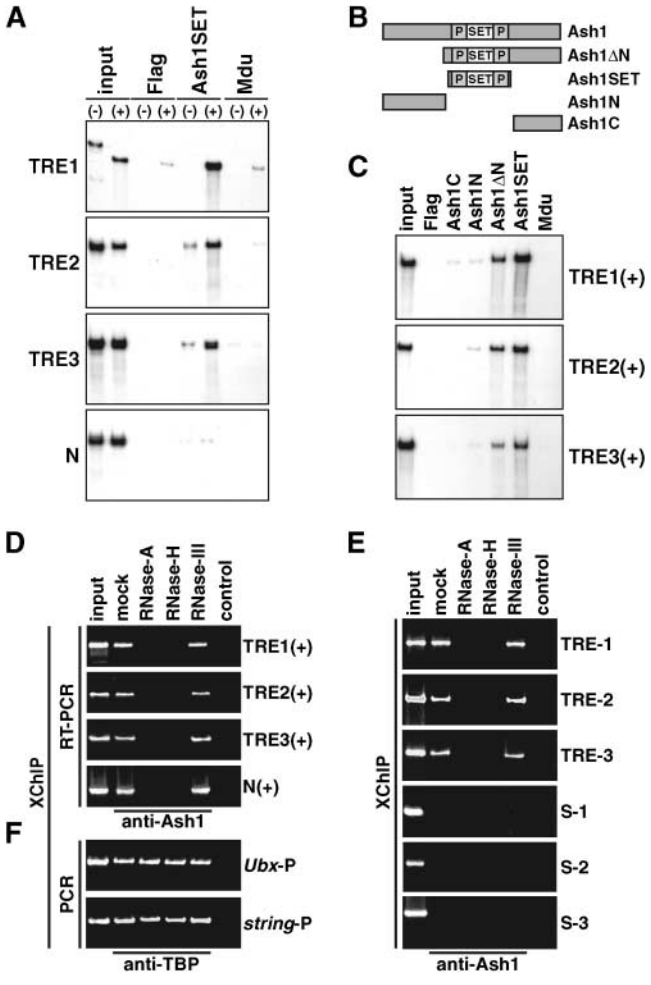

Fig. 3. The SET domain of Ash1 binds TRE transcripts in vitro and in chromatin. (**A**) Autoradiograms of in vitro protein-RNA binding assays (*19*). Radiolabeled sense (+) and antisense (–) transcripts of TRE-1, TRE-2, N, and TRE-3 were incubated with anti-Flag M2 antibody agarose (Flag) or Flag beads loaded with recombinant Ash1SET or Medusa (Mdu). (**B**) Schematic representation of Ash1 and truncated Ash1 derivatives. The position of the SET domain (SET) and pre- and post-SET domains (P) are indicated. (**C**) In vitro protein-RNA binding assays as in (A), except that Flag beads were loaded with Ash1SET, Ash1ΔN, Ash1C, or Ash1N (amino acids 1 to 1001). In (A) and (C), input represents 10% of the input RNA. (**D**) PCR analysis of XChIP immunoprecipitates detecting the association of Ash1 with *bxd* transcripts in mock and RNase-treated and subsequently cross-linked chromatin isolated from third-leg discs. (**E**) XChIP assays were used to detect the association of Ash1 with TREs in chromatin. (**F**) XChIP assays were used to detect the association of TBP to the *Ubx* promoter (*Ubx*-P) and *string/cdc25* promoter (*string*-P) in precipitated DNA pools. In (D) to (F), input represents DNA and RNA detected in 0.5% of the input material.

interacts with the TATA box in eukaryotic promoters (*25*). PCR detected the interaction of TBP with the promoter of *Ubx* and *string*, whose transcription requires TFIID activity (*26*). TBP interacted with both promoters in mock-treated and RNase A–, RNase H–, and RNase III–treated chromatin, indicating that RNase treatment did not attenuate TBP-promoter interactions and protein-gene interactions in general (Fig. 3F) (fig. S7).

To test whether the detected association of Ash1 with TREs and TRE transcripts occurs in chromatin or is the result of fortuitous interactions generated in chemically cross-linked chromatin, we investigated the association of Ash1 with TRE transcripts and TREs in native chromatin with the use of native chromatin immunoprecipitation (NChIP). Ash1 bound all three TREs and TRE transcripts in mock- and RNase III–treated chromatin but not in RNase H– or RNase A–treated chromatin, indicating that Ash1 coimmunoprecipitates with TREs and TRE transcripts in native chromatin (Fig. 4, A and B) (fig. S8). An association of Ash1 with the N portion of the TRE2(+) transcript, as observed in cross-linked chromatin, was not detectable in native chromatin; this result indicates that, as in vitro, Ash1 binds the RNA corresponding to TRE-2 but not the N region of the TRE2(+) transcript.

Collectively, our data indicate that the recruitment of Ash1 to the TREs of *Ubx* is mediated by RNA and suggests the existence of a trimeric protein–nucleic acid complex in chromatin, consisting of Ash1, TREs, and TRE transcripts.

Ash1 is detectable at about 150 loci on *Drosophila* polytene chromosomes (*10*). To assess whether RNA facilitates Ash1 recruitment to target loci other than *Ubx*, we compared the interaction of Ash1 with target loci on

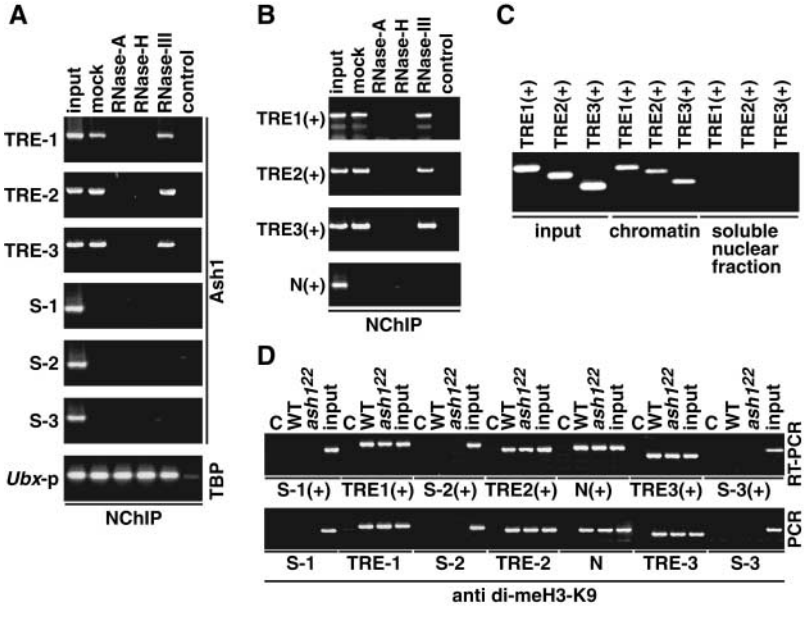

Fig. 4. TRE transcripts mediate the recruitment of Ash1 to *Ubx* TREs in third-leg imaginal discs. (**A**) PCR analysis of NChIP assays detecting the association of Ash1 with *bxd* DNA elements in mock- and RNase-treated chromatin isolated from third-leg imaginal discs. (**B**) RT-PCR analyses of NChIP immunoprecipitates detecting the association of Ash1 with TRE transcripts in native chromatin. (**C**) RT-PCR analyses of NChIP assays detecting the association of Ash1 with TRE transcripts in chromatin and the soluble, histone-free nuclear extract. (**D**) RT-PCR analysis of XChIP RNA immunoprecipitates detecting chromatin-associated *bxd* transcripts (top) and the corresponding *bxd* DNA templates (bottom) in chromatin isolated from wild-type (WT) and *ash1*^{22} mutant third-leg discs. Chromatin was immunoprecipitated with antibodies to dimethylated H3-K9 or rat serum (C). In all panels, input represents the amount of TREs and TRE transcripts detected in 0.5% of the starting material.

mock- and RNase-treated chromosome squashes. Compared to mock-treated chromosomes, RNase treatment attenuated the association of Ash1 with the majority of the target loci (fig. S9). This result suggests that RNA plays an important role in the recruitment of Ash1 to target genes in chromatin.

Ash1 associates with chromatin-bound TRE transcripts. To assess whether TRE transcripts associate with chromatin, we investigated whether Ash1 coprecipitates TRE transcripts from chromatin-free nuclear extract. Ash1 bound TRE transcripts in chromatin but not chromatin-free nuclear extract (Fig. 4C) (fig. S8), indicating that TRE transcripts are preferentially associated with chromatin in the cell.

We used XChIP to determine whether the association of Ash1 with TRE transcripts precedes the recruitment of Ash1 to TREs in chromatin, or vice versa. In vivo cross-linked chromatin was isolated from wild-type and *ash1*^{22} mutant third-leg discs, sheared, and immunoprecipitated with antibodies to dimethylated H3-K9 present at the TREs of the transcriptionally active and inactive *Ubx* locus in third-leg discs (Fig. 2, A and B). The antibody to dimethylated H3-K9 coprecipitated with TREs and TRE transcripts from the chromatin of wild-type and *ash1*^{22} third-leg discs (Fig. 4D) (fig. S10), indicating that TRE transcripts are retained at *Ubx* TREs before recruitment of Ash1.

TRE transcripts recruit Ash1 in trans. To dissect the role of TRE transcripts in *Ubx* transcription, we asked whether transiently transcribed TRE transcripts could restore the recruitment of Ash1 to *Ubx* TREs and *Ubx* expression in S2 cells, which express Ash1 but lack endogenous TRE transcripts. S2 cells were transiently transfected with plasmids transcribing sense or antisense TRE transcripts (*19*) (Fig. 5A) (fig. S11). In PCR assays, *Ubx* transcription was undetectable in S2 cells transiently transcribing antisense TRE transcripts or *mdu* (Fig. 5, A and B). In contrast, *Ubx* transcription was activated by one TRE transcript (Fig. 5B) (fig. S11) and cooperatively activated by multiple TRE transcripts (fig. S12).

We next used XChIP to determine whether activation of *Ubx* transcription by transient TRE transcripts coincides with the recruitment of Ash1 to TREs. In vivo cross-linked chromatin was isolated from wild-type S2 cells and cells transiently transcribing one or multiple TRE transcripts and control RNAs, and it was then immunoprecipitated with antibodies to Ash1 and the Ash1 histone methylation pattern (Fig. 5C). Ash1 was not detected at the TREs of transcriptionally silent *Ubx* in cells transcribing *mdu* or antisense TRE RNAs (Fig. 5C). In contrast, Ash1 and the Ash1 histone methylation pattern were detected at the *Ubx* TREs in cells transcribing TRE1(+), TRE2(+), and/or TRE3(+) (Fig. 5C) (fig. S13). Each of the three TRE transcripts facilitated the association of Ash1 only with the corresponding template TRE but not with other TREs.

To verify the specificity of the described recruitment, we investigated whether TRE transcripts facilitate recruitment of Ash1 to CMEs containing TREs/PREs and genes other than *Ubx*. In XChIP assays, Ash1 was not detected at *Drosophila* genes and the CMEs *MCP* and *Fab7* in S2 cells transcribing TRE1(+), TRE2(+), or TRE3(+) (fig. S14) (*12*, *13*). Thus, TRE transcripts facilitate Ash1 recruitment specifically to the corresponding TRE template DNA.

We used NChIP and XChIP to assess whether transiently transcribed TRE transcripts associate with TREs and Ash1 in chromatin. Native chromatin was isolated from wild-type S2 cells and S2 cells transiently cotranscribing all three sense or antisense TRE transcripts. Ash1 did not associate with TRE transcripts (Fig. 5, D and F) and TREs (Fig. 5, E and G) in cross-linked (Fig. 5, D and E) and native chromatin (Fig. 5, F and G) from S2 cells transcribing *mdu*. In contrast, Ash1 interacted with TREs and TRE transcripts in S2 cells cotranscribing TRE1(+), TRE2(+), and TRE3(+) (Fig. 5, D to G) (fig. S11).

The association of Ash1 with TREs and TRE transcripts was attenuated by RNase A and RNase H but not RNase III (Fig. 5, D to G) (fig. S11). RNase treatment did not abolish the association of TBP with the *Ubx* promoter (Fig. 5, E and G). These results indicate that Ash1 associates with TRE transcripts and TREs in vivo and that TRE transcripts mediate the association of Ash1 with TREs in trans.

To test this hypothesis, we used RNA interference (RNAi) to assess whether degradation of TRE transcripts attenuates recruitment of Ash1 to *Ubx* TREs and *Ubx* expression in third-leg discs (*27*). In vitro cultivated third-leg discs were incubated with small interfering RNAs (siRNAs) targeting all three TRE transcripts or with control siRNA. RT-PCR and XChIP assays indicated that siRNA-mediated degradation of TRE transcripts attenuates *Ubx* transcription and the interaction of Ash1 with TREs (Fig. 6, A and B) (fig. S15).

Next, we used the binary Gal4/UAS system to determine whether ectopic transcription of TRE transcripts restores recruitment of Ash1 to *Ubx* TREs and *Ubx* transcription (*28*). Effector flies carrying a heat-inducible driver (hsp70Gal4) were crossed with reporter flies carrying Gal4-dependent reporter genes (UAS-TRE) consisting of Gal4-responsive UAS DNA sites and a promoter driving the transcription of

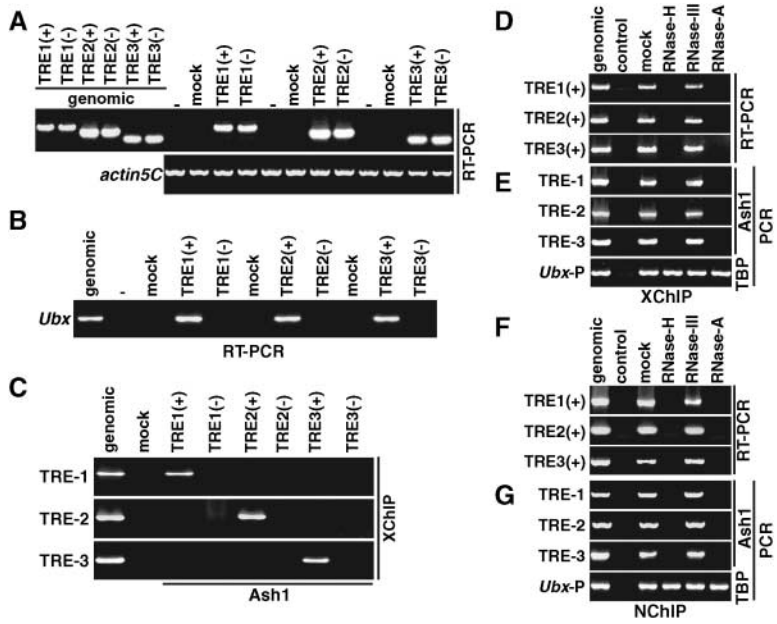

Fig. 5. TRE transcripts reconstitute the interaction of Ash1 with *Ubx* TREs and *Ubx* transcription in S2 cells. (**A**) PCR analysis detecting TRE transcripts and *actin5C* transcription in wild-type S2 cells (–) and S2 cells transfected with plasmids transcribing *mdu* (mock), TRE transcripts [TRE1(+), TRE2(+), TRE3(+)], or antisense TRE transcripts [TRE1(–), TRE2(–), TRE3(–)]. (**B**) PCR assays as in (A) but detecting *Ubx* transcription in wild-type and transfected S2 cells. (**C**) PCR analysis of immunoprecipitates detecting the association of Ash1 with *Ubx* TREs in S2 cells transcribing *mdu* (mock) or sense and antisense TRE transcripts. (**D** and **E**) RT-PCR and PCR analyses of immunoprecipitates detecting the association of Ash1 with *Ubx* TRE transcripts (D) and TREs (E) and TBP with the *Ubx* promoter (*Ubx*-P) (E) in chromatin from S2 cells transiently cotranscribing TRE1(+), TRE2(+), and TRE3(+). (**F** and **G**) RT-PCR (F) and XChIP assays (G) as in (D) and (E), except that native chromatin was used. Transcripts and DNA elements detected in *Drosophila* genomic DNA are also shown.

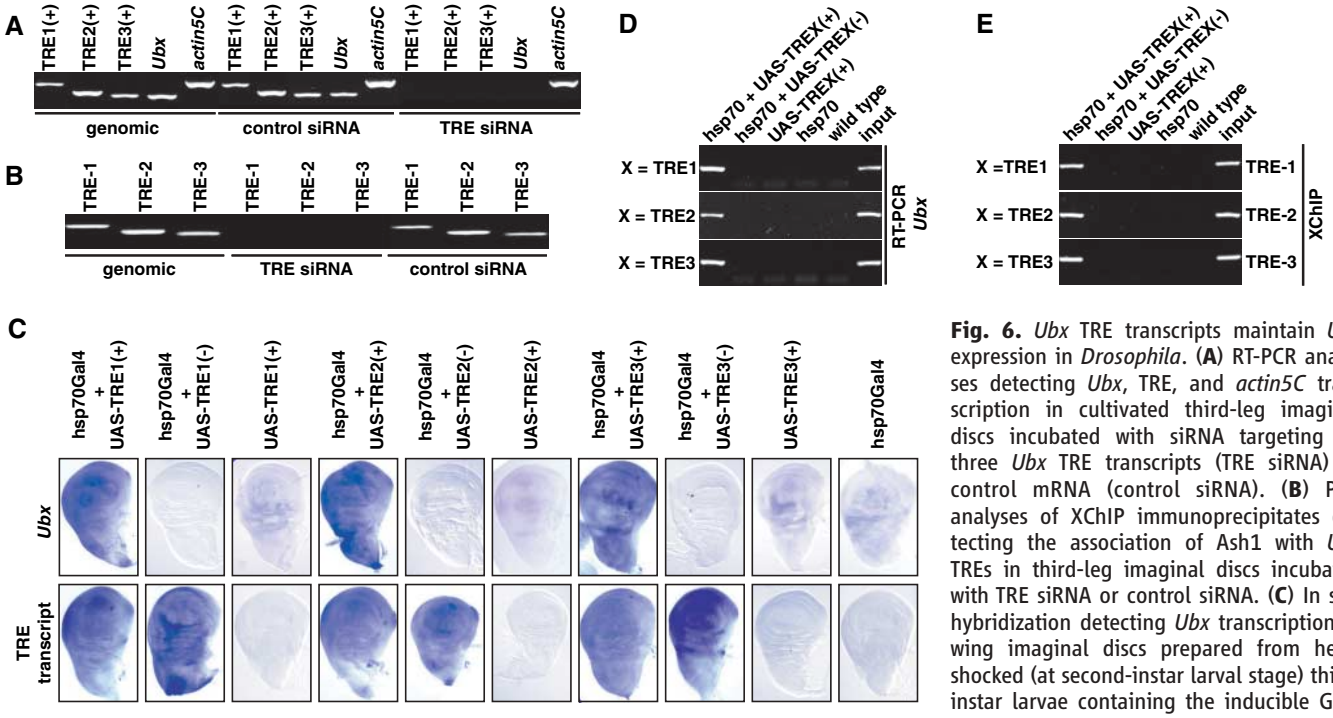

Fig. 6. *Ubx* TRE transcripts maintain *Ubx* expression in *Drosophila*. (**A**) RT-PCR analyses detecting *Ubx*, TRE, and *actin5C* transcription in cultivated third-leg imaginal discs incubated with siRNA targeting all three *Ubx* TRE transcripts (TRE siRNA) or control mRNA (control siRNA). (**B**) PCR analyses of XChIP immunoprecipitates detecting the association of Ash1 with *Ubx* TREs in third-leg imaginal discs incubated with TRE siRNA or control siRNA. (**C**) In situ hybridization detecting *Ubx* transcription in wing imaginal discs prepared from heat-shocked (at second-instar larval stage) third-instar larvae containing the inducible Gal4 driver (hsp70Gal4) and/or Gal4-dependent reporter plasmids (UAS-TRE) transcribing sense (+) or antisense (–) *Ubx* TRE transcripts. (**D**) RT-PCR analyses detecting *Ubx* transcription in wing imaginal discs described in (C). (**E**) PCR analyses of XChIP immunoprecipitates detecting the association of Ash1 with *Ubx* TREs in wing imaginal discs described in (C).

sense and antisense TRE transcripts. Heat treatment of second-instar larvae resulted in ectopic transcription of TRE transcripts in all imaginal discs of third-instar larvae. Ectopic transcription of each TRE transcript nucleated ectopic transcription of *Ubx* in wing imaginal discs (Fig. 6, C and D) (figs. S15 and S16) and facilitated the recruitment of Ash1 to the corresponding *Ubx* TREs (Fig. 6E). It is noteworthy that ectopic TRE transcription in second-instar larvae caused lethality in pupae. In contrast, ectopic *Ubx* expression was not observed in discs prepared from heat-treated parental strains and discs transcribing antisense TRE transcripts (Fig. 6C).

Transcription of antisense TRE transcripts attenuated endogenous transcription of *Ubx* in wing discs isolated from young third-instar larvae, which suggests that ectopic transcription of antisense RNA interferes with the TRE transcript–mediated recruitment of Ash1 to *Ubx* TREs. In summary, our data provide evidence that noncoding TRE transcripts facilitate activation of *Ubx* expression by recruiting Ash1 to the *Ubx* TREs in the fly.

Discussion. Noncoding RNAs play an important role in the recruitment of proteins in several epigenetic phenomena. Recent studies have linked siRNAs to heterochromatin formation and transcriptional silencing of transgenes and transposons (*29*, *30*). SiRNAs facilitate the recruitment of HMTs and DNA methyltransferases to chromatin (*31*, *32*). In *Schizosaccharomyces pombe*, heterochromatic silencing involves the RNA-induced initiator of transcriptional gene silencing complex (RITS), which contains an siRNA component that is essential for the recruitment of RITS to heterochromatic loci (*31*). The inability of RNase III, the key enzyme of the RNAi machinery, to degrade TRE transcripts into siRNAs and the interaction of Ash1 with full-length TRE transcripts in chromatin strongly argues against the involvement of siRNAs in the described RNA-dependent recruitment of Ash1 to chromatin.

Long ncRNAs are key players in imprinting and gene dosage compensation (*22*, *27*, *33*). In *Drosophila*, gene dosage compensation is achieved by a global twofold up-regulation of transcription from the male X chromosome and depends on the activity of the dosage compensation complex (DCC) that contains male-specific proteins and two ncRNAs, *RNA on X 1* (*rox1*) and *RNA on X 2* (*rox2*) (*20*). Both RNAs are transcribed by single-copy genes that, as well as several other X chromosome regions, serve as chromatin entry sites for the DCC on paternal X chromosomes (*20*, *27*). *Rox1* and *Rox2* facilitate the assembly and recruitment of the DCC to chromatin entry sites (*20*). In mammals, spreading of *Xist* RNA culminates in X chromosome inactivation (*22*). Current models propose that the association between ncRNAs and chromatin involves their interaction with proteins, nascent transcripts at template DNA, or the template DNA (*27*, *34*). The observed attenuation of the association between TRE transcripts and TREs by RNase H suggests that TRE transcripts are retained at TREs through hybridization with the corresponding template DNA. Because none of the known DNA repair systems targets DNA-RNA hybrids, RNA-DNA hybrids represent stable molecular entities that, in general, may anchor ncRNAs at corresponding DNA templates in chromatin (*35*).

The three TRE transcripts of *Ubx* do not share common sequence motifs. This is not surprising, because the functionally redundant *rox* RNAs and functionally identical regions in *Xist*, which are required for chromatin localization and protein recruitment, lack identifiable sequence motifs (*27*). Because many RNA-protein interactions are facilitated by RNA secondary structures, the interaction of Ash1 with TRE transcripts might be mediated by secondary RNA structures rather than sequence motifs. In addition, the specificity of RNA-protein interactions is often generated by induced-fit mechanisms that involve complex, extensive conformational changes in both proteins and the target RNA generating a specific interaction surface (*36*, *37*).

Rox1 and *rox2* RNAs transcribed from autosomes can localize to and mediate gene dosage compensation on the male X chromosome, indicating that the chromatin entry of *rox* RNAs does not depend on transcription of chromatin entry sites in cis (*38*). Thus, the association of transiently transcribed TRE transcripts with TREs in S2 cells suggests that TREs function as chromatin entry sites for the corresponding TRE transcripts in trans and cis, and that the transcription and

chromatin entry site activities of TREs are functionally separated. Cumulatively, our results support a model in which RNAs transcribed from the TREs of *Ubx* are retained at TREs through DNA-RNA interactions and provide a RNA scaffold that is bound by Ash1.

References and Notes

1. R. Jaenisch, A. Bird, *Nat. Genet.* **33** (suppl.), 245 (2003).
2. B. M. Turner, *Cell* **111**, 285 (2002).
3. V. Orlando, *Cell* **112**, 599 (2003).
4. L. Ringrose, R. Paro, *Annu. Rev. Genet.* **38**, 413 (2004).
5. A. Breiling, V. Orlando, *Nat. Struct. Biol.* **9**, 894 (2002).
6. P. B. Becker, W. Horz, *Annu. Rev. Biochem.* **71**, 247 (2002).
7. T. Jenuwein, C. D. Allis, *Science* **293**, 1074 (2001).
8. R. Cao, Y. Zhang, *Curr. Opin. Genet. Dev.* **2**, 155 (2004).
9. C. Beisel, A. Imhof, J. Greene, E. Kremmer, F. Sauer, *Nature* **419**, 857 (2002).
10. N. Tripoulas, D. LaJeunesse, J. Gildea, A. Shearn, *Genetics* **143**, 913 (1996).
11. D. LaJeunesse, A. Shearn, *Mech. Dev.* **53**, 123 (1995).
12. S. Schmitt, M. Prestel, R. Paro, *Genes Dev.* **19**, 697 (2005).
13. G. Rank, M. Prestel, R. Paro, *Mol. Cell. Biol.* **22**, 8026 (2002).
14. E. Bae, V. C. Calhoun, M. Levine, E. B. Lewis, R. A. Drewell, *Proc. Natl. Acad. Sci. U S A.* **99**, 16847 (2002).
15. H. D. Lipshitz, D. A. Peattie, D. S. Hogness, *Genes Dev.* **1**, 307 (1987).
16. J. Dejardin *et al.*, *Nature* **434**, 533 (2005).
17. T. Rozovskaia *et al.*, *Mol. Cell. Biol.* **19**, 6441 (1999).
18. C. H. Martin *et al.*, *Proc. Natl. Acad. Sci. USA* **92**, 8398 (1995).
19. See supporting material on *Science* Online.
20. A. Akhtar, *Curr. Opin. Genet. Dev.* **13**, 161 (2003).
21. A. Wutz, *Bioessays* **25**, 434 (2003).
22. E. Heard, *Curr. Opin. Cell Biol.* **16**, 247 (2004).
23. M. A. Matzke, J. A. Birchler, *Nat. Rev. Genet.* **6**, 24 (2005).
24. W. A. Krajewski, T. Nakamura, A. Mazo, E. Canaani, *Mol. Cell. Biol.* **25**, 1891 (2005).
25. S. R. Albright, R. Tjian, *Gene* **242**, 1 (2000).
26. T. Maile, S. Kwoczynski, R. J. Katzenberger, D. A. Wassarman, F. Sauer, *Science* **304**, 1010 (2004).
27. H. Kawasaki, K. Taira, *Curr. Opin. Mol. Ther.* **7**, 125 (2005).
28. C. B. Phelps, A. H. Brand, *Methods* **14**, 367 (1998).
29. E. J. Sontheimer, *Nat. Rev. Mol. Cell Biol.* **6**, 127 (2005).
30. V. Schranke, R. Allshire, *Curr. Opin. Gen. Gev.* **14**, 174 (2004).
31. A. Verdel *et al.*, *Science* **303**, 672 (2004); published online 2 January 2004 (10.1126/science.1093686).
32. M. J. O'Neill, *Hum. Mol. Genet.* **14** Spec No 1:R113 (2004).
33. S. W.-L. Chan *et al.*, *Science* **303**, 1336 (2004).
34. S. I. Grewal, J. C. Rice, *Curr. Opin. Cell Biol.* **16**, 230 (2004).
35. M. Christmann, M. T. Tomicic, W. P. Roos, B. Kaina, *Toxicology* **193**, 3 (2003).
36. Y. Chen, G. Varani, *FEBS J.* **272**, 2088 (2005).
37. F. H. Allain, P. W. Howe, D. Neuhaus, G. Varani, *EMBO J.* **16**, 5764 (1997).
38. V. H. Meller, B. P. Rattner, *EMBO J.* **21**, 1084 (2002).

39. We thank J. A. Diaz-Pendon, E. Poon, and M. Rubalcava for support with RACE, tissue culture, and disc preparation, and members of the Sauer lab for helpful comments that improved the manuscript. F.S. thanks S. Angle for support. Supported by Deutsche Forschungsgemeinschaft (DFG) research fellowship SA1010/1-1 (T.S.-E.), a DFG/Transregio-5 grant (E.K.), and NIH grant GM073776 and VolkswagenStiftung grant I/79-725 (F.S.).

Supporting Online Material

www.sciencemag.org/cgi/content/full/311/5764/1118/DC1
Materials and Methods
Figs. S1 to S16
Tables S1 to S3
References

20 July 2005; accepted 23 January 2006
10.1126/science.1117705

A Swimming Mammaliaform from the Middle Jurassic and Ecomorphological Diversification of Early Mammals

Qiang Ji,[1,3] Zhe-Xi Luo,[2,1]* Chong-Xi Yuan,[3] Alan R. Tabrum[2]

A docodontan mammaliaform from the Middle Jurassic of China possesses swimming and burrowing skeletal adaptations and some dental features for aquatic feeding. It is the most primitive taxon in the mammalian lineage known to have fur and has a broad, flattened, partly scaly tail analogous to that of modern beavers. We infer that docodontans were semiaquatic, convergent to the modern platypus and many Cenozoic placentals. This fossil demonstrates that some mammaliaforms, or proximal relatives to modern mammals, developed diverse locomotory and feeding adaptations and were ecomorphologically different from the majority of generalized small terrestrial Mesozoic mammalian insectivores.

The Middle Jurassic mammalian diversification gave rise to several emergent clades: basal eutriconodontans, amphitheriid cladotherians, the basal mammalian lineage of shuotheriids, and basal australosphenidans (*1*–*5*). These new clades of crown Mammalia coexisted with several mammaliaform lineages (the proximal relatives to modern mammals) (*1*, *6*–*8*). Docodontans are a Mesozoic mammaliaform lineage that have specialized molars for omnivorous feeding; several taxa are known from the Middle Jurassic (*1*, *9*–*13*). Here, we report on a large docodontan mammaliaform that has some dental features for feeding on aquatic invertebrates and small vertebrates, plus specialized skeletal and soft-tissue features for swimming and burrowing.

Description and comparison. *Castorocauda lutrasimilis*, gen. et sp. nov. (*14*), is from the Middle Jurassic Jiulongshan Formation, dated to be approximately 164 million years ago (*15*–*17*). The fauna includes pterosaurs (*17*, *18*), a coelurosaurian dinosaur (*19*), lissamphibians (*20*), abundant fossil insects (*21*), and the conchostracan *Euestheria* (*22*). The holotype of *C. lutrasimilis* (Fig. 1) is represented by a partial skeleton (preserved rostrum-tail length ≥425 mm) with incomplete cranium (preserved length ≥60 mm) but well-preserved mandibles and lower dentition (incisors 4, canine 1, premolars 5, molars 6). Lower molars 3 to 6 have the diagnostic characteristics of docodontans (Fig. 2): anteriorly placed and enlarged lingual cusp g, triangulated crests formed by cusps a-c and a-g, and two partially enclosed basins formed respectively by cusps a, b, and g, and by cusps a, c, and d (*9*–*12*). As in all docodontans, the molars were capable of both shearing by the triangulated crests and grinding between the anterior (''pseudotalonid'') basin and the transversely widened upper molars (*9*–*12*). *Castorocauda* is distinctive from other docodontans in having mediolaterally compressed crowns of molars 1 and 2, each with five cusps in straight alignment (*23*, *24*); primary cusp a and posterior cusps c and d are slightly recurved (Fig. 2). These ''triconodont-like'' anterior molars are plesiomorphic for mammaliaforms (*6*–*8*) but nonetheless distinctive among docodontans. They are convergent to those of placental mesonychians and Eocene whales (*25*). This type of molar with recurved cusps in alignment is hypothesized to be a specialization for feeding on fish and aquatic invertebrates by functional analogy to the teeth of modern pinniped carnivores such as seals.

Castorocauda is preserved with intact middle ear bones (Fig. 2) on the mandible, including the articular (malleus), the surangular, and the angular (ectotympanic). The middle ear bones in anatomical association with the mandible corroborate a previous interpretation of the middle ear in docodontans (*26*). A concavity on the

[1]Department of Earth Science, Nanjing University, Nanjing 200017, China. [2]Carnegie Museum of Natural History, Pittsburgh, PA 15213, USA. [3]Chinese Academy of Geological Sciences, Beijing 100037, China.

*To whom correspondence should be addressed. E-mail: LuoZ@CarnegieMNH.org

RETRACTION

Post date 30 May 2014

Science has received the results of the University of California, Riverside Committee on Privilege and Tenure's investigation of the papers published in *Science* by Professor Frank Sauer and colleagues, "TAF1 activates transcription by phosphorylation of serine 33 in histone H2B" (*1*) and "Noncoding RNAs of trithorax response elements recruit *Drosophila* Ash1 to Ultrabithorax" (*2*).

For the 2004 Report (*1*), the Committee's findings can be summarized as follows: Lanes 3 and 4 in Fig. 1B were replicated from a figure in another paper (*3*). There was manipulation of gel images that constituted data falsification and fabrication in Fig. 2C; Fig. 3, B and C; Fig. 4, B and D; and panel A in fig. S5C.

For the 2006 Research Article (*2*), the Committee's findings can be summarized as follows: In Fig 6C, there was replication of the same image in two panels that constitutes data falsification. There was manipulation of gel images that constituted data falsification and fabrication in Fig. 4D; Fig. 6, A and B; and fig. S5A.

The Committee concluded that the image manipulations described above constituted a significant departure from the accepted practices of Dr. Sauer's research community. Therefore, the data, results, and conclusions in the papers are clearly not reliable. *Science* is hereby retracting the papers, at the request of University of California, Riverside and Dr. Sauer. The Committee determined that Dr. Sauer was the sole individual responsible for producing the figures.

– MARCIA MCNUTT
Editor-in-Chief

References

1. T. Maile, S. Kwoczynski, R. J. Katzenberger, D. A. Wassarman, F. Sauer, *Science* **304**, 1010 (2004).
2. T. Sanchez-Elsner, D. Gou, E. Kremmer, F. Sauer, *Science* **311**, 1118 (2006).
3. C. Beisel, A. Imhof, J. Greene, E. Kremmer, F. Sauer, *Nature* **419**, 857 (2002).

Noncoding RNAs of Trithorax Response Elements Recruit *Drosophila* Ash1 to Ultrabithorax

Tilman Sanchez-Elsner *et al.*

Science **311**, 1118 (2006);
DOI: 10.1126/science.1117705